

Article

Hydrodynamic Behaviour of a Floating Polygonal Platform Centrally Placed within a Polygonal Ring Structure under Wave Action

Jeong Cheol Park *  and Chien Ming Wang

School of Civil Engineering, University of Queensland, St Lucia, QLD 4072, Australia

* Correspondence: jeongcheol.park@uq.net.au

Abstract: In this paper, a semi-analytical method has been developed for the hydrodynamic analysis of a floating polygonal platform that is centrally placed within a floating polygonal ring structure under wave action. In view to understand the wave interactions inside the ring structure, the formulation considers two cases: when the platform and ring structure oscillate individually, and when they oscillate together under wave action. The polygonal shapes of the floating structures can be created from a parametric equation involving the cosine-type radial perturbation. The formulation and computer code are verified by comparing the results with those obtained from the commercial software ANSYS AQWA. When floating ring structures are used, trapped waves are created in the inner water basin resulting in resonance. The interactions among the trapped waves, inner floating platforms and outer ring structures are investigated by performing parametric studies. By changing the dimensions of the platform and ring structure such as the drafts, the radii of platforms and polygonal shapes, their effects on major hydrodynamic quantities may be understood.

Keywords: 3D hydrodynamic analysis; resonance; floating polygonal structures; wave energy harvesting; cosine-type radial perturbation; eigenfunction expansion method



Citation: Park, J.C.; Wang, C.M. Hydrodynamic Behaviour of a Floating Polygonal Platform Centrally Placed within a Polygonal Ring Structure under Wave Action. *J. Mar. Sci. Eng.* **2022**, *10*, 1430. <https://doi.org/10.3390/jmse10101430>

Academic Editors: Carlos Guedes Soares and Serge Sutulo

Received: 2 September 2022

Accepted: 20 September 2022

Published: 4 October 2022

Publisher's Note: MDPI stays neutral with regard to jurisdictional claims in published maps and institutional affiliations.



Copyright: © 2022 by the authors. Licensee MDPI, Basel, Switzerland. This article is an open access article distributed under the terms and conditions of the Creative Commons Attribution (CC BY) license (<https://creativecommons.org/licenses/by/4.0/>).

1. Introduction

Floating platforms have been used for offshore oil and gas rigging, offshore renewable energy farms, aquaculture farms, floating hotels, floating parks, floating houses and floating entertainment/leisure facilities [1–3]. Floating breakwaters create a sheltered sea space that allows safe operation and maintenance of floating solar farms [4], fish farming [5], ship harbouring [6–8], etc. By placing a floating platform within a floating ring breakwater, one may have a practical solution for operating the aforementioned activities in an open sea. For example, Figure 1 shows a conceptual design of a mega offshore floating fish farm surrounded by a hexagonal floating breakwater in an open ocean. The internal floating hexagonal platform houses the control centre, power production and storage facility, fish processing plant, offices, workers' quarters, etc. Alternatively, the floating ring structure may be designed to trap waves to create a high wave energy environment with the view to harvest wave energy using the piston-like internal floating cylinder, i.e., Wave Energy Converter (WEC) device [9,10].

Garrett [8] determined the wave motion inside a thin-walled bottomless harbour using an analytical method. Mavrakos [11] and Mavrakos [12] extended Garrett [8] study for thick-walled floating bottomless circular cylinders and solved the diffraction and radiation problems, respectively. Later, Mavrakos and Chatjigeorgiou [13] tackled the second-order waves for the same problem in order to improve the inaccuracy of the linear wave potential theory due to the trapped waves in the inner water basin resulting in the highly amplified resonant waves. For two concentric floating circular cylinders, Mavrakos [14] and Mavrakos [15] obtained the wave exciting forces and hydrodynamic coefficients. Mavrakos, et al. [16] addressed tightly moored two concentric floating circular

cylinders under first and second-order waves. Konispoliatis, Mazarakos and Mavrakos [10] presented analytical solutions for an array of Oscillating Water Column (OWC) devices. Each OWC device consists of concentric circular cylinders.

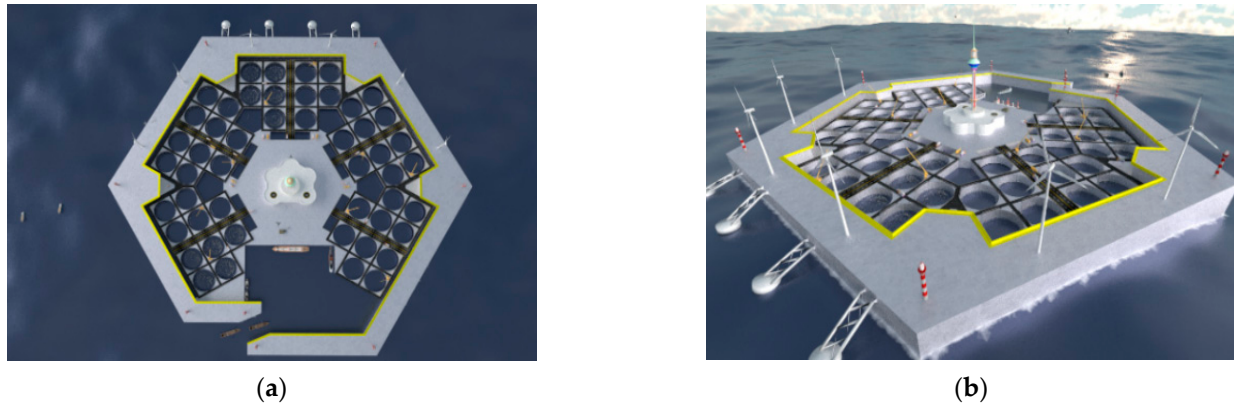


Figure 1. HEXAGON: a mega offshore floating fish farm: (a) plan view; (b) isometric view.

However, the existing formulations are mostly based on floating circular cylinders as it is analytically tractable in the cylindrical coordinate system. In practice, non-circular models are used for marine structure applications [17–19]. Recently, Park and Wang [20] and Park and Wang [21] respectively investigated the hydrodynamic behaviours of floating polygonal platforms and floating polygonal ring structures by solving the diffraction and radiation problems. The shape of the polygonal platform or ring structure was created by using the cosine-type radial perturbation [22]. It has been shown that these hydrodynamic problems can be solved analytically by using the Eigenfunction Expansion Method. In continuing this line of study that uses the analytical method for hydrodynamic analysis of floating structures, this paper further investigates the hydrodynamic behaviour of a floating polygonal platform that is centrally placed within a floating polygonal ring structure. In order to understand the wave interactions inside the ring structure, the study will investigate the cases where the floating platform and ring structure oscillate individually as well as when they oscillate together under wave action. A parametric study involving different drafts, widths of the floating polygonal platforms and polygonal shapes will be performed to understand the hydrodynamic actions inside the floating polygonal ring structure that exhibits resonance phenomena at specific wave frequencies.

The contents of the paper are laid out as follows: Section 2 defines the problem at hand and Section 3 presents the governing equation and boundary conditions for the problem. Section 4 solves the diffracted and radiated potentials by using the semi-analytical approach. Sections 5–7 deal with the determination of the wave exciting forces, hydrodynamic radiation forces and motion responses of the floating platform and ring structure, respectively. Section 8 demonstrates the verification of the present semi-analytical approach by comparing the results with those obtained from the commercial software ANSYS AQWA. Section 9 furnishes the hydrodynamic results for parametric studies. Finally, concluding remarks are given in Section 10.

2. Problem Definition

Consider a floating rigid regular polygonal platform that is centrally placed within a floating rigid regular polygonal ring structure as shown in Figure 2. They are allowed to oscillate together or individually but are assumed to be kept in place as the current and drift force are not considered in this study. The considered water depth is h and the incident wave, having a period T and amplitude A , impacts the floating platform and ring structure at an oblique angle β . The freeboard is assumed to be sufficiently high to prevent wave overtopping. The drafts of the platform and ring structure are d_1 and d_2 , respectively.

The cylindrical coordinates (r, θ, z) are adopted with the origin at the centre of the regular polygonal platform.

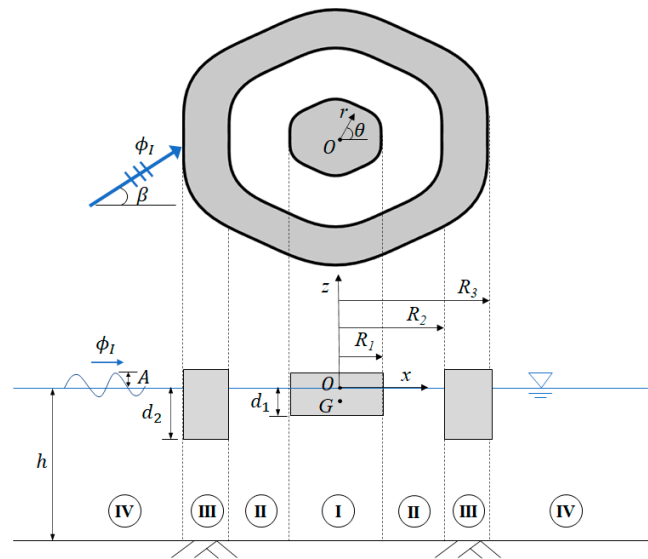


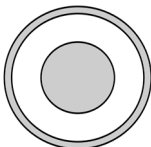
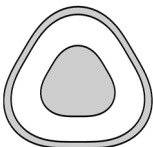
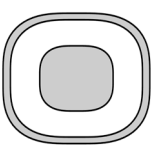
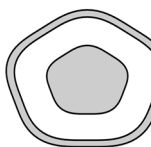
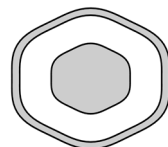
Figure 2. Floating polygonal platform and ring breakwater.

The plan shape of the polygonal platform or polygonal ring structure is generated by using a radius function defined by the cosine-type radial perturbation given by [22]

$$R_l(\theta) = R_{0_l} \{1 + \varepsilon_l \cos n_{p_l}(\theta - \theta_{0_l})\}, \quad l = 1, 2, 3 \tag{1}$$

where $R_{0_l}, \varepsilon_l, n_{p_l}$ and θ_{0_l} are parameters to be chosen by the analyst. This radius function can be used to construct all kinds of regular polygonal shapes. For example, polygonal shapes such as an equilateral triangular, square, pentagon and hexagon can be straightforwardly created by choosing the appropriate values for the dimensionless parameters ε_l, n_{p_l} and θ_{0_l} , which are summarised in Table 1. The size and shape of the polygonal platform and ring structure are predominantly controlled by R_l ($l = 1, 2, 3$) where $l = 1$ represents the platform boundary whilst $l = 2$ and 3 represent the inner and outer boundaries of the ring structure, respectively. In addition, one can freely orientate the polygonal shapes by changing θ_{0_l} .

Table 1. Regular polygonal platform and ring shapes created from the cosine-type radial perturbation S_{0_q} denotes the plan area of the polygonal platform for $q = 1$ and the polygonal ring structure for $q = 2$. The values in the bracket are in turn associated with R_1, R_2 and R_3 .

Polygonal Shapes					
	Circle	Triangle	Square	Pentagon	Hexagon
S_{0_1}	A_{0_1}	$1.005 \times A_{0_1}$	$1.002 \times A_{0_1}$	$1.001 \times A_{0_1}$	$1.000 \times A_{0_1}$
S_{0_2}	A_{0_2}	$1.005 \times A_{0_2}$	$1.002 \times A_{0_2}$	$1.001 \times A_{0_2}$	$1.000 \times A_{0_2}$
ε_l	[0, 0, 0]	[0.1, 0.1, 0.1]	[0.06, 0.06, 0.06]	[0.04, 0.04, 0.04]	[0.03, 0.03, 0.03]
n_{p_l}	[0, 0, 0]	[3, 3, 3]	[4, 4, 4]	[5, 5, 5]	[6, 6, 6]
θ_{0_l}	—	$[\frac{\pi}{2}, \frac{\pi}{2}, \frac{\pi}{2}]$	$[\frac{\pi}{4}, \frac{\pi}{4}, \frac{\pi}{4}]$	$[\frac{\pi}{2}, \frac{\pi}{2}, \frac{\pi}{2}]$	$[\frac{\pi}{6}, \frac{\pi}{6}, \frac{\pi}{6}]$

In this study, the following hydrodynamic properties of floating polygonal platform and ring structure are to be determined: (i) diffracted and radiated potentials, (ii) wave exciting forces, (iii) added mass, (iv) radiation damping, (v) RAOs (Response Amplitude Operators), (vi) wave field.

3. Governing Equation and Boundary Conditions

The hydrodynamic analysis will be performed in the frequency domain. The fluid domain is divided into 4 regions as shown in Figure 2. Region I is the sea space underneath the platform structure, Region II is the sea space between the platform and ring structure, Region III is the sea space underneath the ring structure and Regions IV is the sea space outside the ring structure. The fluid is assumed to be incompressible, inviscid and irrotational, and hence, the linear potential theory may be applied. Accordingly, the fluid motion is governed by the following Laplace equation

$$\frac{1}{r} \frac{\partial}{\partial r} \left(r \frac{\partial \phi}{\partial r} \right) + \frac{1}{r^2} \frac{\partial^2 \phi}{\partial \theta^2} + \frac{\partial^2 \phi}{\partial z^2} = 0 \tag{2}$$

where ϕ is the velocity potential given by

$$\phi = \phi_I + \phi_D + \phi_R \tag{3}$$

in which ϕ_I is the incident potential, ϕ_D the diffracted potential and ϕ_R the radiated potential. The radiated potential may be expressed as the sum of 6 radiation modes corresponding to the six degrees of freedom as

$$\phi_R = \sum_{j=1}^6 \left(-i\omega \xi_j \phi_R^{(j)} \right) \tag{4}$$

where i is the imaginary unit, ω the wave angular frequency, ξ_j the motion amplitude of the ring structure for the j -th radiation mode and $\phi_R^{(j)}$ the normalised radiated potential for the j -th radiation mode.

The velocity potential must satisfy the following boundary conditions

$$\left. \frac{\partial \phi}{\partial z} \right|_{z=0} = \frac{\omega^2}{g} \phi \Big|_{z=0} \quad \text{on the free surface} \tag{5}$$

$$\left. \frac{\partial \phi}{\partial z} \right|_{z=-h} = 0 \quad \text{on the seabed} \tag{6}$$

$$\lim_{r \rightarrow \infty} \left(\frac{\partial \phi_{D,R}}{\partial r} - ik\phi_{D,R} \right) = 0 \quad \text{at infinity} \tag{7}$$

$$\nabla \phi_D \cdot \mathbf{n}_{s_l} = -\nabla \phi_I \cdot \mathbf{n}_{s_l} \quad \text{at wetted surface for diffraction problem} \tag{8}$$

$$\nabla \phi_R^{(j)} \cdot \mathbf{n}_{s_l} = \mathbf{n}_j \cdot \mathbf{n}_{s_l} \quad (j = 1, 2, \dots, 6) \quad \text{at wetted surface for radiation problem} \tag{9}$$

where k is the wave number, g the gravitational acceleration and \mathbf{n}_j the generalised motion normal for 6 DOFs (degrees of freedom), i.e., $\mathbf{n}_1 = \mathbf{n}_x$, $\mathbf{n}_2 = \mathbf{n}_y$, $\mathbf{n}_3 = \mathbf{n}_z$, $\mathbf{n}_4 = -(z - z_G)\mathbf{n}_y + (y - y_G)\mathbf{n}_z$, $\mathbf{n}_5 = (z - z_G)\mathbf{n}_x - (x - x_G)\mathbf{n}_z$ and $\mathbf{n}_6 = -(y - y_G)\mathbf{n}_x + (x - x_G)\mathbf{n}_y$, where (x_G, y_G, z_G) are the coordinates of the floating structure's centre of gravity and \mathbf{n}_{s_l} the unit normal vector to the polygonal body surface pointing out of the floating body. In order to consider the polygonal geometries, the surface function $S_l(r, \theta) = r - R_l(\theta)$, ($l = 1, 2, 3$) is introduced and its derivative with respect to θ is defined

as $\frac{\partial S_l}{\partial \theta} = -\frac{\partial R_l(\theta)}{\partial \theta}$ [23]. By using the surface function, the unit normal vector to the wetted body surface pointing to the fluid \mathbf{n}_{s_l} is given by [23]

$$\mathbf{n}_{s_l} = \frac{\nabla S_l(r, \theta)}{|\mathbf{n}_{s_l}|} = \frac{\frac{\partial S_l}{\partial r} \vec{\mathbf{r}} + \frac{1}{r} \frac{\partial S_l}{\partial \theta} \vec{\boldsymbol{\theta}} + \frac{\partial S_l}{\partial z} \vec{\mathbf{z}}}{|\mathbf{n}_{s_l}|} = \frac{1}{\sqrt{1 + \left(\frac{1}{r} \frac{\partial S_l}{\partial \theta}\right)^2}} \left(\vec{\mathbf{r}} + \frac{1}{r} \frac{\partial S_l}{\partial \theta} \vec{\boldsymbol{\theta}} + 0 \vec{\mathbf{z}} \right) \quad (10)$$

where ∇ denotes the del operator in a cylindrical coordinate system for obtaining the gradient of a vector. Thus, the normal velocity on the floating polygonal platform and ring structure wetted surface can be in general calculated by using the divergence operator in the cylindrical coordinate system as

$$\nabla \phi \cdot \mathbf{n}_{s_l} = \frac{1}{\sqrt{1 + \left(\frac{1}{r} \frac{\partial S_l}{\partial \theta}\right)^2}} \left(\frac{\partial \phi}{\partial r} + \frac{1}{r^2} \frac{\partial S_l}{\partial \theta} \frac{\partial \phi}{\partial \theta} \right) \quad (11)$$

4. Solutions for Diffracted and Radiated Potentials

The assumed solutions for the diffraction and radiation problems can be expressed as a unified form as given by

$$\phi_1^{(j,p)} = \phi_{p_1}^{(j,p)} + \sum_{m=-\infty}^{\infty} \left\{ A_{m0}^{(j,p)} \left(\frac{r}{b_1} \right)^{|m|} + \sum_{n=1}^{\infty} A_{mn}^{(j,p)} \frac{I_m(p_n r)}{I_m(p_n b_1)} \cos p_n(z+h) \right\} e^{im\theta} \quad (12)$$

$$\phi_2^{(j,p)} = \sum_{m=-\infty}^{\infty} \left\{ \left[B_{m0}^{(j,p)} J_m(kr) + C_{m0}^{(j,p)} \frac{H_m(kr)}{H_m(ka_1)} \right] \frac{Z_0(z)}{Z_0(0)} + \sum_{n=1}^{\infty} \left[B_{mn}^{(j,p)} \frac{I_m(k_n r)}{I_m(k_n b_2)} + C_{mn}^{(j,p)} \frac{K_m(k_n r)}{K_m(k_n a_1)} \right] \frac{Z_n(z)}{Z_n(0)} \right\} e^{im\theta} \quad (13)$$

$$\begin{aligned} \phi_3^{(j,p)} = \phi_{p_3}^{(j,p)} + D_{00}^{(j,p)} \ln \frac{r}{a_2} + E_{00}^{(j,p)} \ln \frac{b_3}{r} + \sum_{\substack{m=-\infty \\ m \neq 0}}^{\infty} \left\{ D_{m0}^{(j,p)} \left(\frac{r}{b_3} \right)^{|m|} + E_{m0}^{(j,p)} \left(\frac{r}{a_2} \right)^{-|m|} \right\} e^{im\theta} \\ + \sum_{m=-\infty}^{\infty} \sum_{n=1}^{\infty} \left\{ D_{mn}^{(j,p)} \frac{I_m(q_n r)}{I_m(q_n b_3)} + E_{mn}^{(j,p)} \frac{K_m(q_n r)}{K_m(q_n a_2)} \right\} \cos q_n(z+h) e^{im\theta} \end{aligned} \quad (14)$$

$$\phi_4^{(j,p)} = \sum_{m=-\infty}^{\infty} \left\{ F_{m0}^{(j,p)} \frac{H_m(kr)}{H_m(ka_3)} \frac{Z_0(z)}{Z_0(0)} + \sum_{n=1}^{\infty} F_{mn}^{(j,p)} \frac{K_m(k_n r)}{K_m(k_n a_3)} \frac{Z_n(z)}{Z_n(0)} \right\} e^{im\theta} \quad (15)$$

where the superscript j denotes the diffraction when $j = 0$, otherwise the radiation mode for 6 DOFs ($j = 1$ for surge, $j = 2$ for sway, $j = 3$ for heave, $j = 4$ for roll, $j = 5$ for pitch and $j = 6$ for yaw) and the superscript p denotes the oscillating body, i.e., $p = 1$ for the central platform, $p = 2$ for the ring structure, $p = 3$ for the two bodies oscillating monolithically or individually and $p = 0$ for zero-motion to address the diffraction problem. Hence, in order to obtain the solution for the radiation problem, the two cases for $p = 1$ and 2 must be added. $\phi_{p_1}^{(j,p)}$ and $\phi_{p_3}^{(j,p)}$ are respectively the particular solutions for Regions I and III and the vertical eigenfunction Z_n for both Regions II and IV is given by

$$Z_0(z) = \frac{\cosh k(z+h)}{\sqrt{N_0}}, \quad N_0 = \frac{1}{2} \left[1 + \frac{\sinh 2kh}{2kh} \right], \quad (n = 0) \quad (16)$$

$$Z_n(z) = \frac{\cos k_n(z+h)}{\sqrt{N_n}}, \quad N_n = \frac{1}{2} \left[1 + \frac{\sin 2k_n h}{2k_n h} \right], \quad (n = 1, 2, \dots, \infty) \quad (17)$$

$A_{mn}^{(j,p)}$, $B_{mn}^{(j,p)}$, $C_{mn}^{(j,p)}$ and $D_{mn}^{(j,p)}$ are the unknown complex coefficients to be determined; J_m is the Bessel function of the first kind of order m , I_m and K_m are respectively the modified Bessel function of the first and the second kinds of order m ; a_l and b_l are respectively the shortest and the longest distance from the origin to the structure surface along the radial

direction at $r = R_l(\theta)$ ($l = 1, 2, 3$). The wavenumber k , and the vertical eigenvalue k_n for Regions II and IV are given by

$$\frac{\omega^2}{g} - k \tanh k = 0 \tag{18}$$

$$k_0 = -ik, \quad \frac{\omega^2}{g} + k_n \tan k_n = 0 \quad (n = 1, 2, \infty) \tag{19}$$

and vertical eigenvalues p_n and q_n for Regions I and III are respectively given by

$$p_n = \frac{\pi n}{h - d_1} \quad (n = 0, 1, 2, \infty) \tag{20}$$

$$q_n = \frac{\pi n}{h - d_2} \quad (n = 0, 1, 2, \infty) \tag{21}$$

The particular solutions $\phi_{p_1}^{(j,p)}$ and $\phi_{p_3}^{(j,p)}$ are given by

$$\begin{aligned} \phi_{p_1}^{(j,p)}(r, \theta, z) = & -\delta_{0j} \delta_{0p} \phi_I \\ & + \frac{4(z+h)^2 - (1+\delta_{3j})r^2}{8(h-d_1)} \left\{ \delta_{3j} + \delta_{4j} (r \sin \theta - y_{G_p}) - \delta_{5j} (r \cos \theta - x_{G_p}) \right\} \delta_{1p} + \frac{(\delta_{4j} y_{G_p} - \delta_{5j} x_{G_p})r^2}{8(h-d_1)} \end{aligned} \tag{22}$$

$$\begin{aligned} \phi_{p_3}^{(j,p)}(r, \theta, z) = & -\delta_{0j} \delta_{0p} \phi_I \\ & + \frac{4(z+h)^2 - (1+\delta_{3j})r^2}{8(h-d_2)} \left\{ \delta_{3j} + \delta_{4j} (r \sin \theta - y_{G_p}) - \delta_{5j} (r \cos \theta - x_{G_p}) \right\} \delta_{2p} + \frac{(\delta_{4j} y_{G_p} - \delta_{5j} x_{G_p})r^2}{8(h-d_2)} \end{aligned} \tag{23}$$

where δ_{ij} is the Kronecker delta (1 if $i = j$, 0 if $i \neq j$) and (x_{G_p}, y_{G_p}) the horizontal coordinates of the centre of gravity of the oscillating body p . The incident velocity potential in the cylindrical coordinate system is given by

$$\phi_I(r, \theta, z) = -\frac{igA}{\omega} \sum_{m=-\infty}^{\infty} J_m(kr) e^{im(\theta + \frac{\pi}{2} - \beta)} \frac{\cosh k(z+h)}{\cosh kh} \tag{24}$$

The matching conditions for the pressure and velocity continuities are

$$\nabla \phi_2^{(j,p)} \cdot \mathbf{n}_{s_1} = \begin{cases} \left\{ -\delta_{0p} \nabla \phi_I + (\delta_{1p} + \delta_{3p}) \mathbf{n}_j \right\} \cdot \mathbf{n}_{s_1} \\ \nabla \phi_1^{(j,p)} \cdot \mathbf{n}_{s_1} \end{cases} \quad \text{at } r = R_1 \text{ and } \begin{cases} -d_1 \leq z \leq 0 \\ -h \leq z \leq -d_1 \end{cases} \tag{25}$$

$$\phi_{1,p} = \phi_{2,p} \quad \text{at } r = R_1 \text{ and } -h \leq z \leq -d_1 \tag{26}$$

$$\nabla \phi_2^{(j,p)} \cdot \mathbf{n}_{s_2} = \begin{cases} \left\{ -\delta_{0p} \nabla \phi_I + (\delta_{2p} + \delta_{3p}) \mathbf{n}_j \right\} \cdot \mathbf{n}_{s_2} \\ \nabla \phi_3^{(j,p)} \cdot \mathbf{n}_{s_2} \end{cases} \quad \text{at } r = R_2 \text{ and } \begin{cases} -d_2 \leq z \leq 0 \\ -h \leq z \leq -d_2 \end{cases} \tag{27}$$

$$\phi_{3,p} = \phi_{2,p} \quad \text{at } r = R_2 \text{ and } -h \leq z \leq -d_2 \tag{28}$$

$$\nabla \phi_4^{(j,p)} \cdot \mathbf{n}_{s_3} = \begin{cases} \left\{ -\delta_{0p} \nabla \phi_I + (\delta_{2p} + \delta_{3p}) \mathbf{n}_j \right\} \cdot \mathbf{n}_{s_3} \\ \nabla \phi_3^{(j,p)} \cdot \mathbf{n}_{s_3} \end{cases} \quad \text{at } r = R_3 \text{ and } \begin{cases} -d_2 \leq z \leq 0 \\ -h \leq z \leq -d_2 \end{cases} \tag{29}$$

$$\phi_3^{(j,p)} = \phi_4^{(j,p)} \quad \text{at } r = R_3 \text{ and } -h \leq z \leq -d_2 \tag{30}$$

where R_l ($l = 1, 2, 3$) denotes the radius function as defined in Equation (1) and $\mathbf{n}_j \cdot \mathbf{n}_{s_l}$ ($l = 1, 2, 3$) for 6 DOFs is provided in Appendix A.

We consider the horizontal coordinates of the centre of gravity to coincide with the origin, i.e., $(x_{G_1}, y_{G_1}) = (x_{G_2}, y_{G_2}) = (0, 0)$; however, the vertical coordinate of the centre of gravity may not be zero, $z_{G_1} \neq 0$ and $z_{G_2} \neq 0$. The assumed velocity potentials given in Equations (12) and (15) are substituted into the matching conditions given in Equations (25)–(30). This furnishes

$$\begin{aligned} & \sum_{m=-\infty}^{\infty} \sum_{n=0}^{\infty} \left[B_{mn}^{(j,p)} \left\{ R_1^2 \frac{I_{mn}(k_n R_1)}{I_{mn}(k_n b_2)} + im \frac{I_{mn}(k_n R_1)}{I_{mn}(k_n b_2)} S_{1,\theta} \right\} + C_{mn}^{(j,p)} \left\{ R_1^2 \frac{K'_{mn}(k_n R_1)}{K_{mn}(k_n a_1)} + im \frac{K_{mn}(k_n R_1)}{K_{mn}(k_n a_1)} S_{1,\theta} \right\} \right] \frac{Z_n(z)}{Z_n(0)} e^{im\theta} \\ & = (\delta_{0,p} + \delta_{1,p} + \delta_{3,p}) \mathcal{H}_1^{(j)} \end{aligned} \tag{31}$$

$(r = R_1, -d_1 \leq z \leq 0, 0 \leq \theta \leq 2\pi)$

$$\begin{aligned} & \sum_{m=-\infty}^{\infty} \sum_{n=0}^{\infty} \left[B_{mn}^{(j,p)} \left\{ R_1^2 \frac{\mathcal{I}'_{mn}(k_n R_1)}{\mathcal{I}_{mn}(k_n b_2)} + im \frac{\mathcal{I}_{mn}(k_n R_1)}{\mathcal{I}_{mn}(k_n b_2)} S_{1,\theta} \right\} + C_{mn}^{(j,p)} \left\{ R_1^2 \frac{\mathcal{K}'_{mn}(k_n R_1)}{\mathcal{K}_{mn}(k_n a_1)} S_{1,\theta} + im \frac{\mathcal{K}_{mn}(k_n R_1)}{\mathcal{K}_{mn}(k_n a_1)} S_{1,\theta} \right\} \right] \frac{Z_n(z)}{Z_n(0)} e^{im\theta} \\ & - \sum_{m=-\infty}^{\infty} \sum_{n=0}^{\infty} A_{mn}^{(j,p)} \left\{ R_1^2 \frac{\mathcal{I}'_{mn}(p_n R_1)}{\mathcal{I}_{mn}(p_n b_1)} + im \frac{\mathcal{I}_{mn}(p_n R_1)}{\mathcal{I}_{mn}(p_n b_1)} S_{1,\theta} \right\} \cos p_n(z+h) e^{im\theta} \\ & = (\delta_{0,p} + \delta_{1,p} + \delta_{3,p}) \tilde{\mathcal{P}}_1^{(j)} \end{aligned} \tag{32}$$

$$(r = R_1, -h \leq z \leq -d_1, 0 \leq \theta \leq 2\pi)$$

$$\begin{aligned} & \sum_{m=-\infty}^{\infty} \sum_{n=0}^{\infty} \left\{ B_{mn}^{(j,p)} \frac{\mathcal{I}_{mn}(k_n R_1)}{\mathcal{I}_{mn}(k_n b_2)} + C_{mn}^{(j,p)} \frac{\mathcal{K}_{mn}(k_n R_1)}{\mathcal{K}_{mn}(k_n a_1)} \right\} \frac{Z_n(z)}{Z_n(0)} e^{im\theta} - \sum_{m=-\infty}^{\infty} \sum_{n=0}^{\infty} A_{mn}^{(j,p)} \frac{\mathcal{I}_{mn}(p_n R_1)}{\mathcal{I}_{mn}(p_n b_1)} \cos p_n(z+h) e^{im\theta} \\ & = (\delta_{0,p} + \delta_{1,p} + \delta_{3,p}) \tilde{\mathcal{P}}_1^{(j)} \end{aligned} \tag{33}$$

$$(r = R_1, -h \leq z \leq -d_1, 0 \leq \theta \leq 2\pi)$$

$$\begin{aligned} & \sum_{m=-\infty}^{\infty} \sum_{n=0}^{\infty} \left[B_{mn}^{(j,p)} \left\{ R_2^2 \frac{\mathcal{I}'_{mn}(k_n R_2)}{\mathcal{I}_{mn}(k_n b_2)} + im \frac{\mathcal{I}_{mn}(k_n R_2)}{\mathcal{I}_{mn}(k_n b_2)} S_{2,\theta} \right\} + C_{mn}^{(j,p)} \left\{ R_2^2 \frac{\mathcal{K}'_{mn}(k_n R_2)}{\mathcal{K}_{mn}(k_n a_1)} + im \frac{\mathcal{K}_{mn}(k_n R_2)}{\mathcal{K}_{mn}(k_n a_1)} S_{1,\theta} \right\} \right] \frac{Z_n(z)}{Z_n(0)} e^{im\theta} \\ & = (\delta_{0,p} + \delta_{2,p} + \delta_{3,p}) \tilde{\mathcal{H}}_2^{(j)} \end{aligned} \tag{34}$$

$$(r = R_2, -d_2 \leq z \leq 0, 0 \leq \theta \leq 2\pi)$$

$$\begin{aligned} & \sum_{m=-\infty}^{\infty} \sum_{n=0}^{\infty} \left[B_{mn}^{(j,p)} \left\{ R_2^2 \frac{\mathcal{I}'_{mn}(k_n R_2)}{\mathcal{I}_{mn}(k_n b_2)} + im \frac{\mathcal{I}_{mn}(k_n R_2)}{\mathcal{I}_{mn}(k_n b_2)} S_{2,\theta} \right\} + C_{mn}^{(j,p)} \left\{ R_2^2 \frac{\mathcal{K}'_{mn}(k_n R_2)}{\mathcal{K}_{mn}(k_n a_1)} + im \frac{\mathcal{K}_{mn}(k_n R_2)}{\mathcal{K}_{mn}(k_n a_1)} S_{1,\theta} \right\} \right] \frac{Z_n(z)}{Z_n(0)} e^{im\theta} \\ & - \sum_{m=-\infty}^{\infty} \sum_{n=0}^{\infty} \left[D_{mn}^{(j,p)} \left\{ R_2^2 \frac{\mathcal{I}'_{mn}(q_n R_2)}{\mathcal{I}_{mn}(q_n b_3)} + im \frac{\mathcal{I}_{mn}(q_n R_2)}{\mathcal{I}_{mn}(q_n b_3)} S_{2,\theta} \right\} \right. \\ & \left. + E_{mn}^{(j,p)} \left\{ R_2^2 \frac{\mathcal{K}'_{mn}(q_n R_2)}{\mathcal{K}_{mn}(q_n a_2)} + im \frac{\mathcal{K}_{mn}(q_n R_2)}{\mathcal{K}_{mn}(q_n a_2)} S_{2,\theta} \right\} \right] + \cos q_n(z+h) e^{im\theta} = (\delta_{0,p} + \delta_{2,p} + \delta_{3,p}) \tilde{\mathcal{Q}}_2^{(j)} \end{aligned} \tag{35}$$

$$(r = R_2, -h \leq z \leq -d_2, 0 \leq \theta \leq 2\pi)$$

$$\begin{aligned} & \sum_{m=-\infty}^{\infty} \sum_{n=0}^{\infty} \left\{ B_{mn}^{(j,p)} \frac{\mathcal{I}_{mn}(k_n R_2)}{\mathcal{I}_{mn}(k_n b_2)} + C_{mn}^{(j,p)} \frac{\mathcal{K}_{mn}(k_n R_2)}{\mathcal{K}_{mn}(k_n a_1)} \right\} \frac{Z_n(z)}{Z_n(0)} e^{im\theta} \\ & - \sum_{m=-\infty}^{\infty} \sum_{n=0}^{\infty} \left\{ D_{mn}^{(j,p)} \frac{\mathcal{I}_{mn}(q_n R_2)}{\mathcal{I}_{mn}(q_n b_3)} + E_{mn}^{(j,p)} \frac{\mathcal{K}_{mn}(q_n R_2)}{\mathcal{K}_{mn}(q_n a_2)} \right\} \cos q_n(z+h) e^{im\theta} = (\delta_{0,p} + \delta_{2,p} + \delta_{3,p}) \tilde{\mathcal{Q}}_2^{(j)} \end{aligned} \tag{36}$$

$$(r = R_2, -h \leq z \leq -d_2, 0 \leq \theta \leq 2\pi)$$

$$\begin{aligned} & \sum_{m=-\infty}^{\infty} \sum_{n=0}^{\infty} F_{mn}^{(j,p)} \left\{ R_3^2 \frac{\mathcal{K}'_{mn}(k_n R_3)}{\mathcal{K}_{mn}(k_n a_3)} + im \frac{\mathcal{K}_{mn}(k_n R_3)}{\mathcal{K}_{mn}(k_n a_3)} S_{3,\theta} \right\} \frac{Z_n(z)}{Z_n(0)} e^{im\theta} = (\delta_{0,p} + \delta_{2,p} + \delta_{3,p}) \tilde{\mathcal{H}}_3^{(j)} \end{aligned} \tag{37}$$

$$(r = R_3, -d_2 \leq z \leq 0, 0 \leq \theta \leq 2\pi)$$

$$\begin{aligned} & \sum_{m=-\infty}^{\infty} \left[\sum_{n=0}^{\infty} F_{mn}^{(j,p)} \left\{ R_3^2 \frac{\mathcal{K}'_{mn}(k_n R_3)}{\mathcal{K}_{mn}(k_n a_3)} + im \frac{\mathcal{K}_{mn}(k_n R_3)}{\mathcal{K}_{mn}(k_n a_3)} S_{3,\theta} \right\} \frac{Z_n(z)}{Z_n(0)} e^{im\theta} \right] \\ & - \sum_{m=-\infty}^{\infty} \sum_{n=0}^{\infty} \left[D_{mn}^{(j,p)} \left\{ R_3^2 \frac{\mathcal{I}'_{mn}(q_n R_3)}{\mathcal{I}_{mn}(q_n b_3)} + im \frac{\mathcal{I}_{mn}(q_n R_3)}{\mathcal{I}_{mn}(q_n b_3)} S_{3,\theta} \right\} \right. \\ & \left. + E_{mn}^{(j,p)} \left\{ R_3^2 \frac{\mathcal{K}'_{mn}(q_n R_3)}{\mathcal{K}_{mn}(q_n a_2)} + im \frac{\mathcal{K}_{mn}(q_n R_3)}{\mathcal{K}_{mn}(q_n a_2)} S_{3,\theta} \right\} \right] \cos q_n(z+h) e^{im\theta} = (\delta_{0,p} + \delta_{2,p} + \delta_{3,p}) \tilde{\mathcal{Q}}_3^{(j)} \end{aligned} \tag{38}$$

$$(r = R_3, -h \leq z \leq -d_2, 0 \leq \theta \leq 2\pi)$$

$$\begin{aligned} & \sum_{m=-\infty}^{\infty} \sum_{n=0}^{\infty} F_{mn}^{(j,p)} \frac{\mathcal{K}_{mn}(k_n R_3)}{\mathcal{K}_{mn}(k_n a_3)} \frac{Z_n(z)}{Z_n(0)} e^{im\theta} - \sum_{m=-\infty}^{\infty} \sum_{n=0}^{\infty} \left\{ D_{mn}^{(j,p)} \frac{\mathcal{I}_{mn}(q_n R_3)}{\mathcal{I}_{mn}(q_n b_3)} + E_{mn}^{(j,p)} \frac{\mathcal{K}_{mn}(q_n R_3)}{\mathcal{K}_{mn}(q_n a_2)} \right\} \cos q_n(z+h) e^{im\theta} \\ & = (\delta_{0,p} + \delta_{2,p} + \delta_{3,p}) \tilde{\mathcal{Q}}_3^{(j)} \end{aligned} \tag{39}$$

$$(r = R_3, -h \leq z \leq -d_2, 0 \leq \theta \leq 2\pi)$$

where $S_{l,\theta}$ denotes $\left. \frac{\partial S_l}{\partial \theta} \right|_{r=R_l(\theta)}$ ($l = 1, 2, 3$), \mathcal{K}'_{mn} and \mathcal{I}'_{mn} are respectively the derivatives of \mathcal{K}_{mn} and \mathcal{I}_{mn} with respect to r . $\mathcal{I}_{mn}(k_n r)$, $\mathcal{I}_{mn}(p_n r)$, $\mathcal{I}_{mn}(q_n r)$, $\mathcal{K}_{mn}(q_n r)$ and $\mathcal{K}_{mn}(k_n r)$ are given by

$$\mathcal{I}_{mn}(k_n r) = \begin{cases} J_m(kr) & \text{for } n = 0 \\ \frac{I_m(k_n r)}{I_m(k_n b_2)} & \text{for } n > 0 \end{cases} \tag{40}$$

$$\mathcal{I}_{mn}(p_n r) = \begin{cases} \left(\frac{r}{b_1}\right)^{|m|} & \text{for } n = 0 \\ \frac{I_m(p_n r)}{I_m(p_n b_1)} & \text{for } n > 0 \end{cases} \tag{41}$$

$$\mathcal{I}_{mn}(q_n r) = \begin{cases} \ln \frac{r}{a_2} & \text{for } n = 0 \text{ and } m = 0 \\ \left(\frac{r}{b_3}\right)^{|m|} & \text{for } n = 0 \text{ and } m \neq 0 \\ \frac{I_m(q_n r)}{I_m(q_n b_2)} & \text{for } n > 0 \end{cases} \tag{42}$$

$$\mathcal{K}_{mn}(q_n r) = \begin{cases} \ln \frac{b_3}{r} & \text{for } n = 0 \text{ and } m = 0 \\ \left(\frac{r}{a_2}\right)^{-|m|} & \text{for } n = 0 \text{ and } m \neq 0 \\ \frac{K_m(q_n r)}{K_m(q_n b_2)} & \text{for } n > 0 \end{cases} \tag{43}$$

$$\mathcal{K}_{mn}(k_n r) = \begin{cases} \frac{H_m(kr)}{H_m(ka_3)} & \text{for } n = 0 \\ \frac{K_m(k_n r)}{K_m(k_n a_3)} & \text{for } n > 0 \end{cases} \quad (44)$$

$\mathcal{H}_l^{(j)} \mathcal{P}_l^{(j)}, \mathcal{Q}_l^{(j)}, \tilde{\mathcal{P}}_l^{(j)}$ and $\tilde{\mathcal{Q}}_l^{(j)}$ ($j = 0, 1, \dots, 6; l = 1, 2, 3$) are provided in Appendix B.

In the foregoing formulation, numerical integration should be used for establishing the associated simultaneous equations because the radius functions are substituted into the arguments of radial terms such as the Bessel function, modified Bessel function and radial polynomial functions. Liu, et al. [24] replaced such radial terms with the Fourier expansion series so that the integration could be performed analytically. Recently, Park and Wang [20] suggested an improved method that enables the computational time to be significantly reduced by using minimal numbers of Fourier coefficient sets. By using Park and Wang [20] improved method, 13 sets of Fourier coefficients such as $a_{m,n,q}^{(1)}, b_{m,n,q}^{(1),(2)}, c_{m,n,q}^{(1),(2)}, d_{m,n,q}^{(2),(3)}, e_{m,n,q}^{(2),(3)}, f_{m,q}^{(3)}$ and $g_{m,q}^{(1,2,3)}$ are introduced for solving diffraction and radiation problems. The applied Fourier expansions are as given in Table 2 and their derivatives with respect to r can be directly obtained by using the formerly obtained Fourier coefficients (see Table 3). The Fourier coefficients can be calculated by the functional orthogonality, i.e., by multiplying $e^{-iq\theta}$ and integrating over $[0, 2\pi]$.

Table 2. Fourier expansions for the functions used in velocity potential.

Velocity Potential	Condition	Functions Used	r	Fourier Expansions			
ϕ_1	$n = 0$	Incoming waves	$r^{ m }$	R_1	$\sum_{q=-\infty}^{\infty} a_{m,n,q}^{(1)} e^{iq\theta}$		
	$n > 0$		$I_m(p_n r)$				
ϕ_2	$n = 0$	Incoming waves	$J_m(kr)$	$R_{1,2}$	$\sum_{q=-\infty}^{\infty} b_{m,n,q}^{(1,2)} e^{iq\theta}$		
	$n > 0$		$I_m(k_n r)$				
	$n = 0$	Outgoing waves	$H_m(kr)$		$\sum_{q=-\infty}^{\infty} c_{m,n,q}^{(1,2)} e^{iq\theta}$		
	$n > 0$		$K_m(k_n r)$				
ϕ_3	$n = 0, m = 0$	Incoming waves	$\ln \frac{r}{a_2}$	$R_{2,3}$	$\sum_{q=-\infty}^{\infty} d_{m,n,q}^{(2,3)} e^{iq\theta}$		
	$n = 0, m \neq 0$		$r^{ m }$				
	$n > 0$		$I_m(q_n r)$				
	$n = 0, m = 0$		$\ln \frac{b_3}{r}$				
	$n = 0, m \neq 0$		Outgoing waves			$r^{- m }$	$\sum_{q=-\infty}^{\infty} e_{m,n,q}^{(2,3)} e^{iq\theta}$
	$n > 0$		$K_m(q_n r)$				
ϕ_4	$n = 0$	Outgoing waves	$H_m(k_n r)$	R_1	$\sum_{q=-\infty}^{\infty} f_{m,n,q}^{(1)} e^{iq\theta}$		
	$n > 0$		$K_m(k_n r)$				
ϕ_I	N/A	Incident waves	$J_m(kr)$	$R_{1,2,3}$	$\sum_{q=-\infty}^{\infty} g_{m,n,q}^{(1,2,3)} e^{iq\theta}$		

Table 3. Fourier expansions for the derivative of functions used in velocity potential.

Derivative of Velocity Potential	Condition	Functions Used	r	Fourier Expansions
$\frac{\partial \phi_1}{\partial r}$	$n = 0$	$ m r^{ m -1}$	R_1	$\frac{ m }{r} \sum_{q=-\infty}^{\infty} a_{m,0,q}^{(1)} e^{iq\theta}$
	$n > 0$	$I'_m(p_n r)$		$\frac{p_n}{2} \sum_{q=-\infty}^{\infty} (a_{m-1,n,q}^{(1)} + a_{m+1,n,q}^{(1)}) e^{iq\theta}$
$\frac{\partial \phi_2}{\partial r}$	$n = 0$	$J'_m(kr)$	$R_{1,2}$	$\frac{k}{2} \sum_{q=-\infty}^{\infty} (b_{m-1,0,q}^{(1,2)} - b_{m+1,0,q}^{(1,2)}) e^{iq\theta}$
	$n > 0$	$I'_m(k_n r)$		$\frac{k_n}{2} \sum_{q=-\infty}^{\infty} (b_{m-1,n,q}^{(1,2)} + b_{m+1,n,q}^{(1,2)}) e^{iq\theta}$
	$n = 0$	$H'_m(kr)$		$\frac{k}{2} \sum_{q=-\infty}^{\infty} (c_{m-1,0,q}^{(1,2)} - c_{m+1,0,q}^{(1,2)}) e^{iq\theta}$
	$n > 0$	$K'_m(k_n r)$		$-\frac{k_n}{2} \sum_{q=-\infty}^{\infty} (c_{m-1,n,q}^{(1,2)} + c_{m+1,n,q}^{(1,2)}) e^{iq\theta}$
$\frac{\partial \phi_3}{\partial r}$	$n = 0, m = 0$	$\ln \frac{r}{a_2}$	$R_{2,3}$	$\sum_{q=-\infty}^{\infty} d_{0,0,q}^{(2,3)} e^{iq\theta}$
	$n = 0, m \neq 0$	$r^{ m }$		$\frac{ m }{r} \sum_{q=-\infty}^{\infty} d_{m,0,q}^{(2,3)} e^{iq\theta}$
	$n > 0$	$I_m(q_n r)$		$\frac{q_n}{2} \sum_{q=-\infty}^{\infty} (d_{m-1,n,q}^{(2,3)} + d_{m+1,n,q}^{(2,3)}) e^{iq\theta}$
	$n = 0, m = 0$	$\ln \frac{b_3}{r}$		$-\sum_{q=-\infty}^{\infty} e_{0,0,q}^{(2,3)} e^{iq\theta}$
	$n = 0, m \neq 0$	$r^{- m }$		$-\frac{ m }{r} \sum_{q=-\infty}^{\infty} e_{m,0,q}^{(2,3)} e^{iq\theta}$
	$n > 0$	$K_m(q_n r)$		$-\frac{q_n}{2} \sum_{q=-\infty}^{\infty} (e_{m-1,n,q}^{(2,3)} + e_{m+1,n,q}^{(2,3)}) e^{iq\theta}$
$\frac{\partial \phi_4}{\partial r}$	$n = 0$	$H'_m(k_n r)$	R_3	$\frac{k}{2} \sum_{q=-\infty}^{\infty} (f_{m-1,0,q}^{(3)} - f_{m+1,0,q}^{(3)}) e^{iq\theta}$
	$n > 0$	$K'_m(k_n r)$		$-\frac{k_n}{2} \sum_{q=-\infty}^{\infty} (f_{m-1,n,q}^{(3)} + f_{m+1,n,q}^{(3)}) e^{iq\theta}$
$\frac{\partial \phi_1}{\partial r}$	N/A	Incident waves	$R_{1,2,3}$	$\frac{k}{2} \sum_{q=-\infty}^{\infty} (g_{m-1,0,q}^{(1,2,3)} - g_{m+1,0,q}^{(1,2,3)}) e^{iq\theta}$

Also, the radius function and the derivative of the surface function with respect to θ can be obtained by using $a_{1,0,q}$, $d_{1,0,q}$ and $e_{1,0,q}$.

$$r|_{r=R_1(\theta)} = \sum_{n_r=-\infty}^{\infty} a_{1,0,n_r}^{(1)} e^{in_r\theta} \tag{45}$$

$$r|_{r=R_{2,3}(\theta)} = \sum_{n_r=-\infty}^{\infty} d_{1,0,n_r}^{(2,3)} e^{in_r\theta} \tag{46}$$

$$\frac{1}{r} \Big|_{r=R_{2,3}(\theta)} = \sum_{n_r=-\infty}^{\infty} e_{1,0,n_r}^{(2,3)} e^{in_r\theta} \tag{47}$$

$$\frac{\partial S_1}{\partial \theta} \Big|_{S_1=0} = - \sum_{n_r=-\infty}^{\infty} (in_r) a_{1,0,n_r}^{(1)} e^{in_r\theta} \tag{48}$$

$$\frac{\partial S_{2,3}}{\partial \theta} \Big|_{S_{2,3}=0} = - \sum_{n_r=-\infty}^{\infty} (in_r) d_{1,0,n_r}^{(2,3)} e^{in_r\theta} \tag{49}$$

Equations (31)–(39) can be thus expressed by using the Fourier coefficients obtained in Tables 2 and 3 as

$$\sum_{m=-\infty}^{\infty} \sum_{n_r=-\infty}^{\infty} \sum_{q=-\infty}^{\infty} e^{i(m+n_r+q)\theta} \sum_{n=0}^{\infty} \left[B_{mn}^{(j,p)} \tilde{b}_{m,n,q}^{(1)} + C_{mn}^{(j,p)} \tilde{c}_{m,n,q}^{(1)} \right] \frac{Z_n(z)}{Z_n(0)} = (\delta_{0,p} + \delta_{1,p} + \delta_{3,p}) \mathcal{H}_1^{(j)} \quad (50)$$

$(r = R_1, -d_1 \leq z \leq 0, 0 \leq \theta \leq 2\pi)$

$$\sum_{m=-\infty}^{\infty} \sum_{n_r=-\infty}^{\infty} \sum_{q=-\infty}^{\infty} e^{i(m+n_r+q)\theta} \sum_{n=0}^{\infty} \left[B_{mn}^{(j,p)} \tilde{b}_{m,n,q}^{(1)} + C_{mn}^{(j,p)} \tilde{c}_{m,n,q}^{(1)} \right] \frac{Z_n(z)}{Z_n(0)} - \sum_{m=-\infty}^{\infty} \sum_{n_q=-\infty}^{\infty} \sum_{q=-\infty}^{\infty} e^{i(m+n_r+q)\theta} \sum_{n=0}^{\infty} A_{mn}^{(j,p)} \tilde{a}_{m,n,p}^{(1)}$$

$$= (\delta_{0,p} + \delta_{1,p} + \delta_{3,p}) \tilde{\mathcal{P}}_1^{(j)} \quad (r = R_1, -h \leq z \leq -d_1, 0 \leq \theta \leq 2\pi)$$

$$\sum_{m=-\infty}^{\infty} \sum_{q=-\infty}^{\infty} e^{i(m+q)\theta} \sum_{n=0}^{\infty} \left\{ B_{mn}^{(j,p)} \tilde{b}_{m,n,p}^{(1)} + C_{mn}^{(j,p)} \tilde{c}_{m,n,p}^{(1)} \right\} \frac{Z_n(z)}{Z_n(0)} - \sum_{m=-\infty}^{\infty} \sum_{q=-\infty}^{\infty} e^{i(m+q)\theta} \sum_{n=0}^{\infty} A_{mn}^{(j,p)} \tilde{a}_{m,n,p}^{(1)} \cos p_n(z+h)$$

$$= (\delta_{0,p} + \delta_{1,p} + \delta_{3,p}) \tilde{\mathcal{P}}_1^{(j)} \quad (r = R_1, -h \leq z \leq -d_1, 0 \leq \theta \leq 2\pi)$$

$$\sum_{m=-\infty}^{\infty} \sum_{n_r=-\infty}^{\infty} \sum_{q=-\infty}^{\infty} e^{i(m+n_r+q)\theta} \sum_{n=0}^{\infty} \left[B_{mn}^{(j,p)} \tilde{b}_{m,n,q}^{(2)} + C_{mn}^{(j,p)} \tilde{c}_{m,n,q}^{(2)} \right] \frac{Z_n(z)}{Z_n(0)} = (\delta_{0,p} + \delta_{2,p} + \delta_{3,p}) \mathcal{H}_2^{(j)} \quad (53)$$

$(r = R_2, -d_2 \leq z \leq 0, 0 \leq \theta \leq 2\pi)$

$$\sum_{m=-\infty}^{\infty} \sum_{n_r=-\infty}^{\infty} \sum_{q=-\infty}^{\infty} e^{i(m+n_r+q)\theta} \sum_{n=0}^{\infty} \left[B_{mn}^{(j,p)} \tilde{b}_{m,n,q}^{(2)} + C_{mn}^{(j,p)} \tilde{c}_{m,n,q}^{(2)} \right] \frac{Z_n(z)}{Z_n(0)}$$

$$- \sum_{m=-\infty}^{\infty} \sum_{n_r=-\infty}^{\infty} \sum_{q=-\infty}^{\infty} e^{i(m+n_r+q)\theta} \sum_{n=0}^{\infty} \left[D_{mn}^{(j,p)} \tilde{d}_{m,n,q}^{(2)} + E_{mn}^{(j,p)} \tilde{e}_{m,n,q}^{(2)} \right] \cos q_n(z+h)$$

$$= (\delta_{0,p} + \delta_{2,p} + \delta_{3,p}) \tilde{\mathcal{Q}}_2^{(j)} \quad (r = R_2, -h \leq z \leq -d_2, 0 \leq \theta \leq 2\pi)$$

$$\sum_{m=-\infty}^{\infty} \sum_{q=-\infty}^{\infty} e^{i(m+q)\theta} \sum_{n=0}^{\infty} \left[B_{mn}^{(j,p)} \tilde{b}_{m,n,q}^{(2)} + C_{mn}^{(j,p)} \tilde{c}_{m,n,q}^{(2)} \right] \frac{Z_n(z)}{Z_n(0)}$$

$$- \sum_{m=-\infty}^{\infty} \sum_{q=-\infty}^{\infty} e^{i(m+q)\theta} \sum_{n=0}^{\infty} \left[D_{mn}^{(j,p)} \tilde{d}_{m,n,q}^{(2)} + E_{mn}^{(j,p)} \tilde{e}_{m,n,q}^{(2)} \right] \cos q_n(z+h) = (\delta_{0,p} + \delta_{2,p} + \delta_{3,p}) \tilde{\mathcal{Q}}_2^{(j)}$$

$(r = R_2, -h \leq z \leq -d_2, 0 \leq \theta \leq 2\pi)$

$$\sum_{m=-\infty}^{\infty} \sum_{n_r=-\infty}^{\infty} \sum_{q=-\infty}^{\infty} e^{i(m+n_r+q)\theta} \sum_{n=0}^{\infty} F_{mn}^{(j,p)} \tilde{f}_{m,n,q}^{(3)} \frac{Z_n(z)}{Z_n(0)} = (\delta_{0,p} + \delta_{2,p} + \delta_{3,p}) \mathcal{H}_3^{(j)} \quad (56)$$

$(r = R_3, -d_2 \leq z \leq 0, 0 \leq \theta \leq 2\pi)$

$$\sum_{m=-\infty}^{\infty} \sum_{n_r=-\infty}^{\infty} \sum_{q=-\infty}^{\infty} e^{i(m+n_r+q)\theta} \sum_{n=0}^{\infty} F_{mn}^{(j,p)} \tilde{f}_{m,n,q}^{(3)} \frac{Z_n(z)}{Z_n(0)}$$

$$- \sum_{m=-\infty}^{\infty} \sum_{n_r=-\infty}^{\infty} \sum_{q=-\infty}^{\infty} e^{i(m+n_r+q)\theta} \sum_{n=0}^{\infty} \left[D_{mn}^{(j,p)} \tilde{d}_{m,n,q}^{(3)} + E_{mn}^{(j,p)} \tilde{e}_{m,n,q}^{(3)} \right] \cos q_n(z+h)$$

$$= (\delta_{0,p} + \delta_{2,p} + \delta_{3,p}) \tilde{\mathcal{Q}}_3^{(j)} \quad (r = R_3, -h \leq z \leq -d_2, 0 \leq \theta \leq 2\pi)$$

$$\sum_{m=-\infty}^{\infty} \sum_{q=-\infty}^{\infty} e^{i(m+q)\theta} \sum_{n=0}^{\infty} F_{mn}^{(j,p)} \tilde{f}_{m,n,q}^{(3)} \frac{Z_n(z)}{Z_n(0)} - \sum_{m=-\infty}^{\infty} \sum_{q=-\infty}^{\infty} e^{i(m+q)\theta} \sum_{n=0}^{\infty} \left[D_{mn}^{(j,p)} \tilde{d}_{m,n,q}^{(3)} + E_{mn}^{(j,p)} \tilde{e}_{m,n,q}^{(3)} \right] \cos q_n(z+h)$$

$$= (\delta_{0,p} + \delta_{2,p} + \delta_{3,p}) \tilde{\mathcal{Q}}_3^{(j)} \quad (r = R_3, -h \leq z \leq -d_2, 0 \leq \theta \leq 2\pi)$$

where the reduced forms of $\tilde{a}_{m,n,q}^{(1)}$, $\tilde{b}_{m,n,q}^{(1),(2)}$, $\tilde{c}_{m,n,q}^{(1),(2)}$, $\tilde{d}_{m,n,q}^{(2),(3)}$, $\tilde{e}_{m,n,q}^{(2),(3)}$, $\tilde{f}_{m,n,q}^{(3)}$ and their normal derivatives are given in Appendix C.

By multiplying the corresponding vertical eigenfunctions $\frac{1}{h} Z_n(z)$ in Equations (50), (51), (53), (54), (56) and (57), $\frac{1}{h-d_1} \cos p_n(z+h)$ in Equation (52), $\frac{1}{h-d_2} \cos q_n(z+h)$ in Equations (55) and (58) and the angular eigenfunction $e^{-im\theta}$ in Equations (50)–(58) and integrating the equations for the associated integral intervals, one can combine Equation (50) with (51), Equation (53) with (54) and Equation (56) with (57). By truncating the series terms at $m = M$, $n = N$, $n_r = N_r$ and $q = N_q$, $9(2M+1)(N+1)$ equations for the monolithic motion or $18(2M+1)(N+1)$ equations for the individual motion, and the same number

of unknowns are given for the diffraction problem and each radiation mode. Consequently, the unknown complex coefficients ($A_{mn}^{(j,p)}$, $B_{mn}^{(j,p)}$, $C_{mn}^{(j,p)}$, $D_{mn}^{(j,p)}$, $E_{mn}^{(j,p)}$, $F_{mn}^{(j,p)}$) can be solved by linear algebra.

5. Determination of Wave Exciting Force

From Bernoulli’s equation, the fluid pressure p is given by

$$p = \rho i \omega \phi \tag{59}$$

where ρ is the water density.

By integrating over the wetted areas, the wave exciting force and rotational moment for 6 DOFs are obtained by

$$F_{w_j}^{(q)} = \rho i \omega \int_{S_{w_q}} (\phi_I + \phi_D) \cdot \mathbf{n}_j dS_{w_q} \tag{60}$$

where S_{w_q} denotes the wetted surface of the floating body q on which the wave exciting forces are acting.

By substituting the incident velocity potential and diffracted potentials with obtained unknown complex coefficients into Equation (60), the wave exciting forces in 3 DOFs (i.e., surge, heave and pitch) acting on the floating polygonal platform ($q = 1$) and ring structure ($q = 2$) are given below:

$$\begin{aligned} F_{w_1}^{(1)} &= \rho i \omega \int_0^{2\pi} \int_{-d_1}^0 (\phi_I + \phi_{D_2})|_{r=R_1} R_1 \mathbf{n}_x \cdot (-\mathbf{n}_{s_1}) dz d\theta \\ &= \frac{\rho g A}{\cosh kh} \sum_{m=-\infty}^{\infty} e^{im(\frac{\pi}{2}-\beta)} \int_0^{2\pi} J_m(kR_1) e^{im\theta} R_1 \mathbf{n}_1 \cdot (-\mathbf{n}_{s_1}) d\theta \int_{-d_1}^0 \cosh k(z+h) dz \\ &\quad + \rho i \omega \sum_{m=-\infty}^{\infty} \sum_{n=0}^{\infty} \int_0^{2\pi} \{B_{mn} \mathcal{I}_{mn}(k_n R_1) + C_{mn} \mathcal{K}_{mn}(k_n R_2)\} e^{im\theta} R_1 \mathbf{n}_1 \cdot (-\mathbf{n}_{s_1}) d\theta \int_{-d_1}^0 \frac{Z_n(z)}{Z_n(0)} dz \end{aligned} \tag{61}$$

$$\begin{aligned} F_{w_3}^{(1)} &= \rho i \omega \int_0^{2\pi} \int_{R_1}^{R_2} (\phi_I + \phi_{D_2})|_{z=-d_1} \mathbf{n}_z \cdot (\mathbf{n}_z) r dr d\theta \\ &= \rho i \omega \sum_{m=-\infty}^{\infty} \sum_{n=0}^{\infty} \cos p_n (h - d_1) \int_0^{2\pi} \int_0^{R_1} A_{mn} \mathcal{I}_{mn}(p_n r) e^{im\theta} r dr d\theta \end{aligned} \tag{62}$$

$$\begin{aligned} F_{w_5}^{(1)} &= \rho i \omega \int_0^{2\pi} \left[\int_{-d_1}^0 (z - z_{G_1}) (\phi_I + \phi_{D_2})|_{r=R_1} R_1 \mathbf{n}_x \cdot (-\mathbf{n}_{s_1}) dz - \int_0^{R_1} (\phi_I + \phi_{D_1})|_{z=-d_1} (r \cos \theta) \mathbf{n}_z \cdot (\mathbf{n}_z) r dr \right] d\theta \\ &= \frac{\rho g A}{\cosh kh} \sum_{m=-\infty}^{\infty} e^{im(\frac{\pi}{2}-\beta)} \left[\int_0^{2\pi} J_m(kR_1) R_1 \mathbf{n}_1 \cdot (-\mathbf{n}_{s_1}) e^{im\theta} d\theta \int_{-d_1}^0 (z - z_{G_1}) \cosh k(z+h) dz \right. \\ &\quad \left. - \cosh k(h - d_1) \int_0^{2\pi} \int_0^{R_1} J_m(kr) e^{im\theta} r^2 \cos \theta dr d\theta \right] \\ &\quad + \rho i \omega \sum_{m=-\infty}^{\infty} \sum_{n=0}^{\infty} \left[\int_0^{2\pi} \{B_{mn} \mathcal{I}_{mn}(k_n R_1) + C_{mn} \mathcal{K}_{mn}(k_n R_1)\} e^{im\theta} R_1 \mathbf{n}_1 \cdot (-\mathbf{n}_{s_1}) d\theta \int_{-d_1}^0 (z - z_{G_1}) \frac{Z_n(z)}{Z_n(0)} dz \right. \\ &\quad \left. - \cos p_n (h - d_1) \int_0^{2\pi} \int_0^{R_1} A_{mn} \mathcal{I}_{mn}(p_n r) e^{im\theta} r^2 \cos \theta dr d\theta \right] \end{aligned} \tag{63}$$

$$\begin{aligned} F_{w_1}^{(2)} &= \rho i \omega \int_0^{2\pi} \int_{-d_2}^0 \{ (\phi_I + \phi_{D_2})|_{r=R_2} R_2 \mathbf{n}_x \cdot \mathbf{n}_{s_2} + (\phi_I + \phi_{D_4})|_{r=R_3} R_3 \mathbf{n}_x \cdot (-\mathbf{n}_{s_3}) \} dz d\theta \\ &= \frac{\rho g A}{\cosh kh} \sum_{m=-\infty}^{\infty} e^{im(\frac{\pi}{2}-\beta)} \int_0^{2\pi} \{J_m(kR_2) R_2 \mathbf{n}_1 \cdot \mathbf{n}_{s_2} + J_m(kR_3) R_3 \mathbf{n}_1 \cdot (-\mathbf{n}_{s_3})\} e^{im\theta} d\theta \int_{-d_2}^0 \cosh k(z+h) dz \\ &\quad + \rho i \omega \sum_{m=-\infty}^{\infty} \sum_{n=0}^{\infty} \int_0^{2\pi} \{B_{mn} \mathcal{I}_{mn}(k_n R_2) + C_{mn} \mathcal{K}_{mn}(k_n R_2)\} R_2 \mathbf{n}_1 \cdot \mathbf{n}_{s_2} + F_{mn} \mathcal{K}_{mn}(k_n R_3) R_3 \mathbf{n}_1 \cdot (-\mathbf{n}_{s_3}) e^{im\theta} d\theta \int_{-d_2}^0 \frac{Z_n(z)}{Z_n(0)} dz \end{aligned} \tag{64}$$

$$\begin{aligned} F_{w_3}^{(2)} &= \rho i \omega \int_0^{2\pi} \int_{R_2}^{R_3} (\phi_I + \phi_{D_3})|_{z=-d_2} \mathbf{n}_z \cdot (\mathbf{n}_z) r dr d\theta \\ &= \rho i \omega \sum_{m=-\infty}^{\infty} \sum_{n=0}^{\infty} \cos p_n (h - d_2) \int_0^{2\pi} \int_{R_2}^{R_3} \{D_{mn} \mathcal{I}_{mn}(q_n r) + E_{mn} \mathcal{K}_{mn}(q_n r)\} e^{im\theta} r dr d\theta \end{aligned} \tag{65}$$

$$\begin{aligned}
 F_{w_3}^{(2)} &= \rho i \omega \int_0^{2\pi} \left[\int_{-d_2}^0 (z - z_{G_2}) \left\{ (\phi_I + \phi_{D_2}) \Big|_{r=R_2} R_2 \mathbf{n}_x \cdot \mathbf{n}_{s_2} + (\phi_I + \phi_{D_4}) \Big|_{r=R_3} R_3 \mathbf{n}_x \cdot (-\mathbf{n}_{s_3}) \right\} dz \right. \\
 &\quad \left. - \int_{R_2}^{R_3} (\phi_I + \phi_{D_3}) \Big|_{z=-d_2} (r \cos \theta) \mathbf{n}_z \cdot (\mathbf{n}_z) r dr \right] d\theta \\
 &= \frac{\rho g A}{\cosh kh} \sum_{m=-\infty}^{\infty} e^{im(\frac{\pi}{2}-\beta)} \left[\int_0^{2\pi} \{ J_m(kR_2) R_2 \mathbf{n}_1 \cdot \mathbf{n}_{s_2} + J_m(kR_3) R_3 \mathbf{n}_1 \cdot \mathbf{n}_{s_3} \} e^{im\theta} d\theta \int_{-d_2}^0 (z \right. \\
 &\quad \left. - z_{G_2}) \cosh k(z+h) dz - \cosh k(h-d_2) \int_0^{R_3} \int_{R_2} J_m(kr) e^{im\theta} r^2 \cos \theta dr d\theta \right] \tag{66} \\
 &+ \rho i \omega \sum_{m=-\infty}^{\infty} \sum_{n=0}^{\infty} \int_0^{2\pi} \{ B_{mn} \mathcal{I}(k_n R_2) + C_{mn} \mathcal{K}_{mn}(k_n R_2) \} R_2 \mathbf{n}_1 \cdot \mathbf{n}_{s_2} + F_{mn} \mathcal{K}_{mn}(k_n R_3) R_3 \mathbf{n}_1 \\
 &\quad \cdot (-\mathbf{n}_{s_3}) \} e^{im\theta} d\theta \int_{-d_2}^0 (z - z_{G_2}) \frac{Z_n(z)}{Z_n(0)} dz \\
 &- \rho i \omega \sum_{m=-\infty}^{\infty} \sum_{n=0}^{\infty} \cos p_n (h - d_2) \int_0^{2\pi} \int_{R_2}^{R_3} \{ D_{mn} \mathcal{I}_{mn}(q_n r) + E_{mn} \mathcal{K}_{mn}(q_n r) \} e^{im\theta} r^2 \cos \theta dr d\theta
 \end{aligned}$$

where the unknown complex coefficients for the diffraction $A_{mn}^{(0,0)}$, $B_{mn}^{(0,0)}$, $C_{mn}^{(0,0)}$, $D_{mn}^{(0,0)}$, $E_{mn}^{(0,0)}$ and $F_{mn}^{(0,0)}$ are expressed as A_{mn} , B_{mn} , C_{mn} , D_{mn} , E_{mn} and F_{mn} for brevity. z_{G_1} and z_{G_2} are the z-coordinates of the centre of gravity for the floating polygonal platform and ring structure, respectively. The wave exciting forces for other DOFs such as sway, roll and yaw can be similarly obtained by using the unit normal vector $(-\mathbf{n}_s + \mathbf{n}_z)$ and the generalised motion normal \mathbf{n}_j . The divergence $\mathbf{n}_j \cdot \mathbf{n}_s$ are given in Appendix A.

6. Determination of Radiation Forces

The radiation force is obtained by

$$F_{ij}^{(q,p)} = i\omega\rho \int_{S_{wq}} \left\{ -i\omega\tilde{\zeta}_j^{(p)} \phi_R^{(j,p)} \right\} \mathbf{n}_j dS_{wq} = \tilde{\zeta}_j \left(\omega^2 \mu_{ij}^{(q,p)} + i\omega \lambda_{ij}^{(q,p)} \right) \tag{67}$$

where $\mu_{ij}^{(q,p)}$ and $\lambda_{ij}^{(q,p)}$ are the added mass and the radiation damping of the floating body q by the oscillating body p for the i -th mode of force and the j -th mode of motion, which are respectively defined as

$$\mu_{ij}^{(q,p)} = \text{Re} \left(\rho f_{ij}^{(q,p)} \right) \tag{68}$$

$$\lambda_{ij}^{(q,p)} = \text{Im} \left(\rho \omega f_{ij}^{(q,p)} \right) \tag{69}$$

$\text{Re}(\cdot)$ denotes the real part and $\text{Im}(\cdot)$ the imaginary part. $f_{ij}^{(q,p)}$ is the integral form for i -th mode of force and j -th mode of motion associated with the floating body q by the oscillating body p . By substituting the normalised radiated velocity potentials with the obtained unknown complex coefficients into Equation (67), $f_{ij}^{(q,p)}$ ($p = 1, 2$ and $q = 1, 2$) for 3 DOFs are given by

$$\begin{aligned}
 f_{11}^{(1,p)} &= \int_0^{2\pi} \int_{-d_1}^0 \phi_{R_2}^{(1,p)} \Big|_{r=R_1} \mathbf{n}_x \cdot (-\mathbf{n}_{s_1}) R_1 dz d\theta \\
 &= \sum_{m=-\infty}^{\infty} \sum_{n=0}^{\infty} \int_0^{2\pi} \left\{ B_{mn}^{(1,p)} \mathcal{I}_{mn}(k_n R_1) + C_{mn}^{(1,p)} \mathcal{K}_{mn}(k_n R_1) \right\} R_1 \mathbf{n}_x \cdot (-\mathbf{n}_{s_1}) \} e^{im\theta} d\theta \int_{-d_1}^0 \frac{Z_n(z)}{Z_n(0)} dz \tag{70}
 \end{aligned}$$

$$\begin{aligned}
 f_{51}^{(1,p)} &= \int_0^{2\pi} \left\{ \int_{-d_1}^0 (z - z_{G_1}) \phi_{R_2}^{(1,p)} \Big|_{r=R_1} \mathbf{n}_x \cdot (-\mathbf{n}_{s_1}) R_1 dz - \int_0^{R_1} \phi_{R_1}^{(1,p)} \Big|_{z=-d_1} (r \cos \theta) \mathbf{n}_z \cdot (\mathbf{n}_z) r dr \right\} d\theta \\
 &= \sum_{m=-\infty}^{\infty} \sum_{n=0}^{\infty} \int_0^{2\pi} \left\{ B_{mn}^{(1,p)} \mathcal{I}_{mn}(k_n R_1) + C_{mn}^{(1,p)} \mathcal{K}_{mn}(k_n R_1) \right\} R_1 \mathbf{n}_x \cdot (-\mathbf{n}_{s_1}) e^{im\theta} d\theta \int_{-d_1}^0 (z - z_{G_1}) \frac{Z_n(z)}{Z_n(0)} dz \\
 &\quad - \sum_{m=-\infty}^{\infty} \sum_{n=0}^{\infty} \cos p_n (h - d_1) \int_0^{2\pi} \int_0^{R_1} A_{mn}^{(1,p)} \mathcal{I}_{mn}(p_n r) e^{im\theta} r^2 \cos \theta dr d\theta
 \end{aligned} \tag{71}$$

$$\begin{aligned}
 f_{33}^{(1,p)} &= \int_0^{2\pi} \int_0^{R_1} \phi_{R_2}^{(3,p)} \Big|_{z=-d_1} \mathbf{n}_z \cdot (\mathbf{n}_z) r dr d\theta \\
 &= \delta_{1p} \int_0^{2\pi} \int_0^{R_1} \left\{ \frac{(h-d_1)}{2} - \frac{r^2}{4(h-d_1)} \right\} r dr d\theta \\
 &\quad + \sum_{m=-\infty}^{\infty} \sum_{n=0}^{\infty} \cos p_n (h - d_1) \int_0^{2\pi} \int_0^{R_1} A_{mn}^{(3,p)} \mathcal{I}_{mn}(p_n r) e^{im\theta} r dr d\theta
 \end{aligned} \tag{72}$$

$$\begin{aligned}
 f_{55}^{(1,p)} &= \int_0^{2\pi} \left[\int_{-d_1}^0 (z - z_{G_1}) \phi_{R_2}^{(5,p)} \Big|_{r=R_1} \mathbf{n}_x \cdot (-\mathbf{n}_{s_1}) R_1 dz - \int_0^{R_1} \phi_{R_1}^{(5,p)} \Big|_{z=-d_1} (r \cos \theta) \mathbf{n}_z \cdot (\mathbf{n}_z) r dr \right] d\theta \\
 &= \sum_{m=-\infty}^{\infty} \sum_{n=0}^{\infty} \int_0^{2\pi} \left\{ A_{mn}^{(5,p)} \mathcal{I}_{mn}(p_n R_1) e^{im\theta} R_1 \mathbf{n}_x \cdot (-\mathbf{n}_{s_1}) \right\} d\theta \int_{-d_1}^0 (z - z_{G_1}) \frac{Z_n(z)}{Z_n(0)} dz \\
 &\quad - \left\{ \delta_{1p} \int_0^{2\pi} \int_0^{R_1} \frac{-4(h-d_1)^2 + r^2}{8(h-d_1)} r \cos \theta r^2 \cos \theta dr d\theta \right. \\
 &\quad \left. + \sum_{m=-\infty}^{\infty} \sum_{n=0}^{\infty} \cos p_n (h - d_1) \int_0^{2\pi} \int_0^{R_1} A_{mn}^{(5,p)} \mathcal{I}_{mn}(p_n r) e^{im\theta} r^2 \cos \theta dr d\theta \right\}
 \end{aligned} \tag{73}$$

$$\begin{aligned}
 f_{15}^{(1,p)} &= \int_0^{2\pi} \int_{-d_1}^0 \phi_{R_2}^{(5,p)} \Big|_{r=R_1} \mathbf{n}_x \cdot (-\mathbf{n}_{s_1}) R_1 dz d\theta \\
 &= \sum_{m=-\infty}^{\infty} \sum_{n=0}^{\infty} \int_0^{2\pi} \left\{ B_{mn}^{(5,p)} \mathcal{I}_{mn}(k_n R_1) + C_{mn}^{(5,p)} \mathcal{K}_{mn}(k_n R_1) \right\} R_1 \mathbf{n}_x \cdot (-\mathbf{n}_{s_1}) e^{im\theta} d\theta \int_{-d_1}^0 \frac{Z_n(z)}{Z_n(0)} dz
 \end{aligned} \tag{74}$$

$$\begin{aligned}
 f_{11}^{(2,p)} &= \int_0^{2\pi} \int_{-d_2}^0 \left\{ \phi_{R_2}^{(1,p)} \Big|_{r=R_2} \mathbf{n}_x \cdot (\mathbf{n}_{s_2}) R_2 + \phi_{R_4}^{(1,p)} \Big|_{r=R_3} \mathbf{n}_x \cdot (-\mathbf{n}_{s_3}) R_3 \right\} dz d\theta \\
 &= \sum_{m=-\infty}^{\infty} \sum_{n=0}^{\infty} \int_0^{2\pi} \left[\left\{ B_{mn}^{(1,p)} \mathcal{I}_{mn}(k_n R_2) + C_{mn}^{(1,p)} \mathcal{K}_{mn}(k_n R_2) \right\} R_2 \mathbf{n}_x \cdot (\mathbf{n}_{s_2}) + F_{mn}^{(1,p)} \mathcal{K}_{mn}(R_3) R_3 \mathbf{n}_x \right. \\
 &\quad \left. \cdot (-\mathbf{n}_{s_3}) \right] e^{im\theta} d\theta \int_{-d_2}^0 \frac{Z_n(z)}{Z_n(0)} dz
 \end{aligned} \tag{75}$$

$$\begin{aligned}
 f_{51}^{(2,p)} &= \int_0^{2\pi} \left\{ \int_{-d_2}^0 (z - z_{G_2}) \left\{ \phi_{R_2}^{(1,p)} \Big|_{r=R_2} \mathbf{n}_x \cdot (\mathbf{n}_{s_2}) R_2 + \phi_{R_4}^{(1,p)} \Big|_{r=R_3} \mathbf{n}_x \cdot (-\mathbf{n}_{s_3}) R_3 \right\} dz \right. \\
 &\quad \left. - \int_{R_2}^{R_3} \phi_{R_3}^{(1,p)} \Big|_{z=-d_2} (r \cos \theta) \mathbf{n}_z \cdot (\mathbf{n}_z) r dr \right\} d\theta \\
 &= \sum_{m=-\infty}^{\infty} \sum_{n=0}^{\infty} \int_0^{2\pi} \left\{ \left\{ B_{mn}^{(1,p)} \mathcal{I}_{mn}(k_n R_2) + C_{mn}^{(1,p)} \mathcal{K}_{mn}(k_n R_2) \right\} R_2 \mathbf{n}_x \cdot (\mathbf{n}_{s_2}) + F_{mn}^{(1,p)} \mathcal{K}_{mn}(k_n R_3) R_3 \mathbf{n}_x \right. \\
 &\quad \left. \cdot (-\mathbf{n}_{s_3}) \right\} e^{im\theta} d\theta \int_{-d_2}^0 (z - z_{G_2}) \frac{Z_n(z)}{Z_n(0)} dz \\
 &\quad - \sum_{m=-\infty}^{\infty} \sum_{n=0}^{\infty} \cos p_n (h - d_2) \int_0^{2\pi} \int_{R_2}^{R_3} \left\{ D_{mn}^{(1,p)} \mathcal{I}_{mn}(q_n r) + E_{mn}^{(1,p)} \mathcal{K}_{mn}(q_n r) \right\} e^{im\theta} r^2 \cos \theta dr d\theta
 \end{aligned} \tag{76}$$

$$\begin{aligned}
 f_{33}^{(2,p)} &= \int_0^{2\pi} \int_{R_2}^{R_3} \phi_{R_3}^{(3,p)} \Big|_{z=-d_2} \mathbf{n}_z \cdot (\mathbf{n}_z) r dr d\theta \\
 &= \delta_{2p} \int_0^{2\pi} \int_{R_2}^{R_3} \left\{ \frac{(h-d_2)}{2} - \frac{r^2}{4(h-d_2)} \right\} r dr d\theta \\
 &\quad + \sum_{m=-\infty}^{\infty} \sum_{n=0}^{\infty} \cos p_n (h - d_2) \int_0^{2\pi} \int_{R_2}^{R_3} \left\{ D_{mn}^{(3,p)} \mathcal{I}_{mn}(q_n r) + E_{mn}^{(3,p)} \mathcal{K}_{mn}(q_n r) \right\} e^{im\theta} r dr d\theta
 \end{aligned} \tag{77}$$

$$\begin{aligned}
 f_{55}^{(2,p)} &= \int_0^{2\pi} \left[\int_{-d_2}^0 (z - z_{G_2}) \left\{ \phi_{R_2}^{(5,p)} \Big|_{r=R_2} \mathbf{n}_x \cdot (\mathbf{n}_{s_2}) R_2 + \phi_{R_4}^{(5,p)} \Big|_{r=R_3} \mathbf{n}_x \cdot (-\mathbf{n}_{s_3}) R_3 \right\} dz - \int_{R_2}^{R_3} \phi_{R_3}^{(5,p)} \Big|_{z=-d_2} (r \cos \theta) \mathbf{n}_z \cdot (\mathbf{n}_z) r dr \right] d\theta \\
 &= \sum_{m=-\infty}^{\infty} \sum_{n=0}^{\infty} \int_0^{2\pi} \left[\left\{ B_{mn}^{(5,p)} \mathcal{I}_{mn}(k_n R_2) + C_{mn}^{(5,p)} \mathcal{K}_{mn}(k_n R_2) \right\} R_2 \mathbf{n}_x \cdot (\mathbf{n}_{s_2}) + F_{mn}^{(5,p)} \mathcal{K}_{mn}(k_n R_3) R_3 \mathbf{n}_x \cdot (-\mathbf{n}_{s_3}) \right] e^{im\theta} d\theta \int_{-d_2}^0 (z - z_{G_2}) \frac{Z_n(z)}{Z_n(0)} dz \\
 &\quad - \left\{ \delta_{2p} \int_0^{2\pi} \int_{R_2}^{R_3} \frac{-4(h-d_2)^2 + r^2}{8(h-d_2)} r \cos \theta r^2 \cos \theta dr d\theta \right. \\
 &\quad \left. + \sum_{m=-\infty}^{\infty} \sum_{n=0}^{\infty} \cos p_n (h - d_2) \int_0^{2\pi} \int_{R_2}^{R_3} \left\{ D_{mn}^{(5,p)} \mathcal{I}_{mn}(q_n r) + E_{mn}^{(5,p)} \mathcal{K}_{mn}(q_n r) \right\} e^{im\theta} r^2 \cos \theta dr d\theta \right\}
 \end{aligned} \tag{78}$$

$$\begin{aligned}
 f_{15}^{(2,p)} &= \int_0^{2\pi} \int_{-d_2}^0 \left\{ \phi_{R_2}^{(5,p)} \Big|_{r=R_2} \mathbf{n}_x \cdot (\mathbf{n}_{s_2}) R_1 + \phi_{R_4}^{(5,p)} \Big|_{r=R_3} \mathbf{n}_x \cdot (-\mathbf{n}_{s_3}) R_3 \right\} dz d\theta \\
 &= \sum_{m=-\infty}^{\infty} \sum_{n=0}^{\infty} \int_0^{2\pi} \left\{ \left\{ B_{mn}^{(5,p)} \mathcal{I}_{mn}(k_n R_2) + C_{mn}^{(5,p)} \mathcal{K}_{mn}(k_n R_2) \right\} R_2 \mathbf{n}_x \cdot (\mathbf{n}_{s_2}) + F_{mn}^{(5,p)} \mathcal{K}_{mn}(k_n R_3) R_3 \mathbf{n}_x \right. \\
 &\quad \left. \cdot (-\mathbf{n}_{s_3}) \right\} e^{im\theta} d\theta \int_{-d_2}^0 \frac{Z_n(z)}{Z_n(0)} dz
 \end{aligned} \tag{79}$$

Note that $f_{15}^{(q,p)}$ and $f_{51}^{(p,q)}$ are the same when the geometry of the floating body is symmetrical about the x -axis.

7. Motion Responses of Floating Ring Structure

Consider the horizontal coordinates of the centre of gravity of the floating regular polygonal ring structure coincide with the origin, i.e., $(x_{G_1}, y_{G_1}) = (x_{G_2}, y_{G_2}) = (0, 0)$ but $z_{G_1} \neq 0$ and $z_{G_2} \neq 0$. As regular polygons are geometrically symmetrical about certain axes, the products of inertia of the floating regular polygonal platform/structure will become zero regardless of their orientation. If the motion of the floating body is relatively small, the following equations of motion in 3 DOFs (i.e., surge, heave and pitch) are satisfied.

$$\begin{aligned}
 & \left[-\omega^2 (m^{(1)} + \mu_{11}^{(1,1)}) - i\omega \lambda_{11}^{(1,1)} \right] \{ \xi_1^{(1)} \} + \left[-\omega^2 \mu_{15}^{(1,1)} - i\omega \lambda_{15}^{(1,1)} \right] \{ \xi_5^{(1)} \} + \left[-\omega^2 \mu_{11}^{(1,2)} - i\omega \lambda_{11}^{(1,2)} \right] \{ \xi_1^{(2)} \} \\
 & \quad + \left[-\omega^2 \mu_{15}^{(1,2)} - i\omega \lambda_{15}^{(1,2)} \right] \{ \xi_5^{(2)} \} = \{ F_1^{(1)} \}
 \end{aligned} \tag{80}$$

$$\left[-\omega^2 (m^{(1)} + \mu_{33}^{(1,1)}) - i\omega \lambda_{33}^{(1,1)} + \rho g A_w^{(1)} \right] \{ \xi_3^{(1)} \} + \left[-\omega^2 \mu_{33}^{(1,2)} - i\omega \lambda_{33}^{(1,2)} \right] \{ \xi_3^{(2)} \} = \{ F_3^{(1)} \} \tag{81}$$

$$\begin{aligned}
 & \left[-\omega^2 \mu_{51}^{(1,1)} - i\omega \lambda_{51}^{(1,1)} \right] \{ \xi_1^{(1)} \} + \left[-\omega^2 (I_{52}^{(1)} + \mu_{55}^{(1,1)}) - i\omega \lambda_{55}^{(1,1)} + m^{(1)} g \overline{GM}_L^{(1)} \right] \{ \xi_5^{(1)} \} + \left[-\omega^2 \mu_{51}^{(1,2)} - i\omega \lambda_{51}^{(1,2)} \right] \{ \xi_1^{(2)} \} \\
 & \quad + \left[-\omega^2 \mu_{55}^{(1,2)} - i\omega \lambda_{55}^{(1,2)} \right] \{ \xi_5^{(2)} \} = \{ F_5^{(1)} \}
 \end{aligned} \tag{82}$$

$$[-\omega^2(m^{(2)} + \mu_{11}^{(2,2)}) - i\omega\lambda_{11}^{(2,2)}]\{\xi_1^{(2)}\} + [-\omega^2\mu_{15}^{(2,2)} - i\omega\lambda_{15}^{(2,2)}]\{\xi_5^{(2)}\} + [-\omega^2\mu_{11}^{(2,1)} - i\omega\lambda_{11}^{(2,1)}]\{\xi_1^{(1)}\} + [-\omega^2\mu_{15}^{(2,1)} - i\omega\lambda_{15}^{(2,1)}]\{\xi_5^{(1)}\} = \{F_1^{(2)}\} \tag{83}$$

$$[-\omega^2(m^{(2)} + \mu_{33}^{(2,2)}) - i\omega\lambda_{33}^{(2,2)} + \rho g A_w^{(2)}]\{\xi_3^{(2)}\} + [-\omega^2\mu_{33}^{(2,1)} - i\omega\lambda_{33}^{(2,1)}]\{\xi_3^{(1)}\} = \{F_3^{(2)}\} \tag{84}$$

$$[-\omega^2\mu_{51}^{(2,2)} - i\omega\lambda_{51}^{(2,2)}]\{\xi_1^{(2)}\} + [-\omega^2(I_{22}^{(2)} + \mu_{55}^{(2,2)}) - i\omega\lambda_{55}^{(2,2)} + m^{(2)}g\overline{GM}_L^{(2)}]\{\xi_5^{(2)}\} + [-\omega^2\mu_{51}^{(2,1)} - i\omega\lambda_{51}^{(2,1)}]\{\xi_1^{(1)}\} + [-\omega^2\mu_{55}^{(2,1)} - i\omega\lambda_{55}^{(2,1)}]\{\xi_5^{(1)}\} = \{F_5^{(2)}\} \tag{85}$$

where $m^{(p)}$ is the mass of the oscillating body p , $\xi_i^{(p)}$ the unknown displacement of the oscillating body p at i -th radiation mode, $F_i^{(q)}$ the wave exciting force acting on the floating body q , $I_{ii}^{(p)}$ ($i = 1, 2, 3$) the mass moment of inertia of the oscillating body p about i -axis, $A_w^{(p)}$ the waterplane area of the oscillating body p , $V_w^{(p)}$ the wetted volume of the oscillating body p , $\overline{GM}_T^{(p)}$ ($= \frac{A_{w11}^{(p)}}{V_w^{(p)}} + z_B^{(p)} - z_G^{(p)}$) the transverse metacentric height of the oscillating body p , $\overline{GM}_L^{(p)}$ ($= \frac{A_{w22}^{(p)}}{V_w^{(p)}} + z_B^{(p)} - z_G^{(p)}$) the longitudinal metacentric height of the oscillating body p and $A_{wii}^{(p)}$ ($i = 1, 2$) is the second moment over the waterplane area of the oscillating body p about i -axis.

By linear algebra, the motion responses $\xi_i^{(p)}$ ($i = 1, 2, \dots, 6$) are solved by using Equations (80)–(85). By substituting the solutions into Equation (4), one can obtain the radiated potential.

8. Verification of Semi-Analytical Approach and Computer Code

In order to verify the semi-analytical approach and the computer code, we compare the hydrodynamic results (i.e., added mass, radiation damping, wave exciting forces, RAO and wave field) with those obtained from the commercial software ANSYS AQWA based on the Boundary Element Method.

For the verification exercise, we consider a floating hexagonal platform that is placed within a floating hexagonal ring structure whose geometries are defined by the radius function as given in Equation (1) with $R_{01} = 50$ m, $R_{02} = 90$ m, $R_{03} = 100$ m, $\epsilon_{1,2,3} = 0.03$, $n_{p1,2,3} = 6$ and $\theta_{01,2,3} = \frac{\pi}{6}$. The drafts d_1 for the platform and d_2 for the ring structure are equally 10 m. Figure 3 shows the structural shape. It is assumed that the centre of gravity coincides with the origin and the water depth is 50 m. The incident wave is along the x -axis (i.e., $\beta = 0^\circ$).

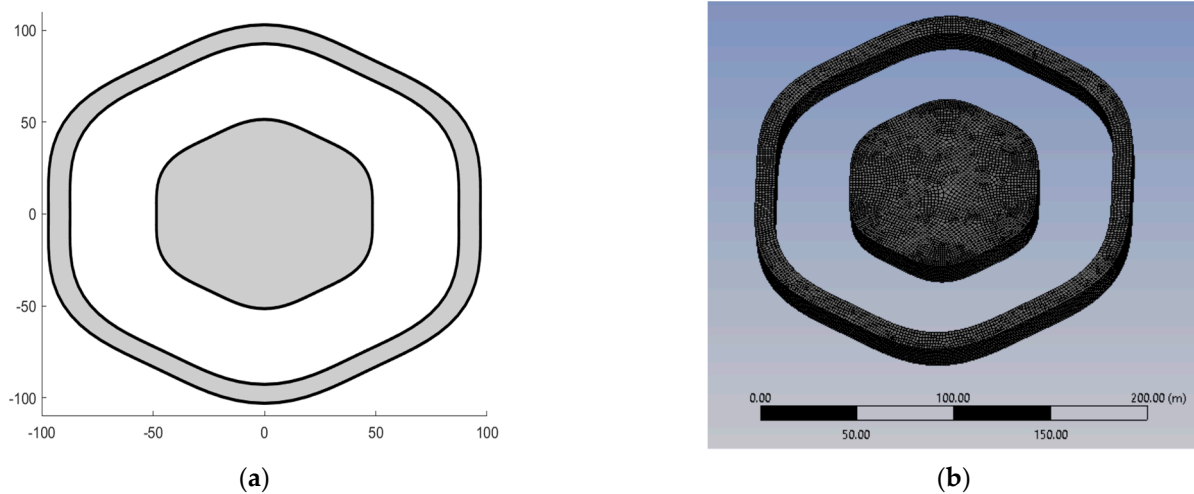


Figure 3. Hexagonal ring structure for verification study: (a) plan view; (b) 3D mesh model (AQWA).

For the 3D model in AQWA, the maximum mesh size is 2.8 m which leads to a total of 11,459 diffracting elements to be used. It should be noted that a fine mesh model is required to obtain a reasonably converged inner free water elevation. The regular wave angular frequency domain for AQWA is divided into 20 frequencies for the interval [0.3866 rad/s, 1.2528 rad/s], which is equivalent to $kh = [1, 8]$.

Figure 4 presents the added mass and radiation damping obtained from the present semi-analytical method and AQWA. The numbers of truncated terms for the present semi-analytical method were taken as $M = 30, N = 5, N_r = 12$ and $N_q = 24$ for parametric studies. It is unnecessary to perform the integration for all the m -series terms, but series index m can be restricted to

$$\begin{aligned}
 m &= \pm 1, \pm(n_p \pm 1) && \text{for surge or sway} \\
 m &= 0, \pm n_p && \text{for heave} \\
 m &= \pm 1, \pm(n_p \pm 1), \pm(2n_p \pm 1) && \text{for roll or pitch} \\
 m &= 0, \pm 2, \pm n_p, \pm(n_p \pm 2), \pm(2n_p \pm 1), \pm 2n_p && \text{for yaw}
 \end{aligned}
 \tag{86}$$

where n_p is the parameter of the radius function as given in Equation (1). Also, it should be noted that N_r and N_q can be taken as multiple numbers of n_p . For instance, $N_r = 12$ and $N_q = 24$ are respectively 2 and 4 times $n_p = 6$ for a hexagonal shape. This rule can be equally applied for calculating the wave exciting forces. Hence, such a selective calculation can speed up the hydrodynamic analysis in composing the global system matrix as well as obtaining the wave exciting forces and radiation forces.

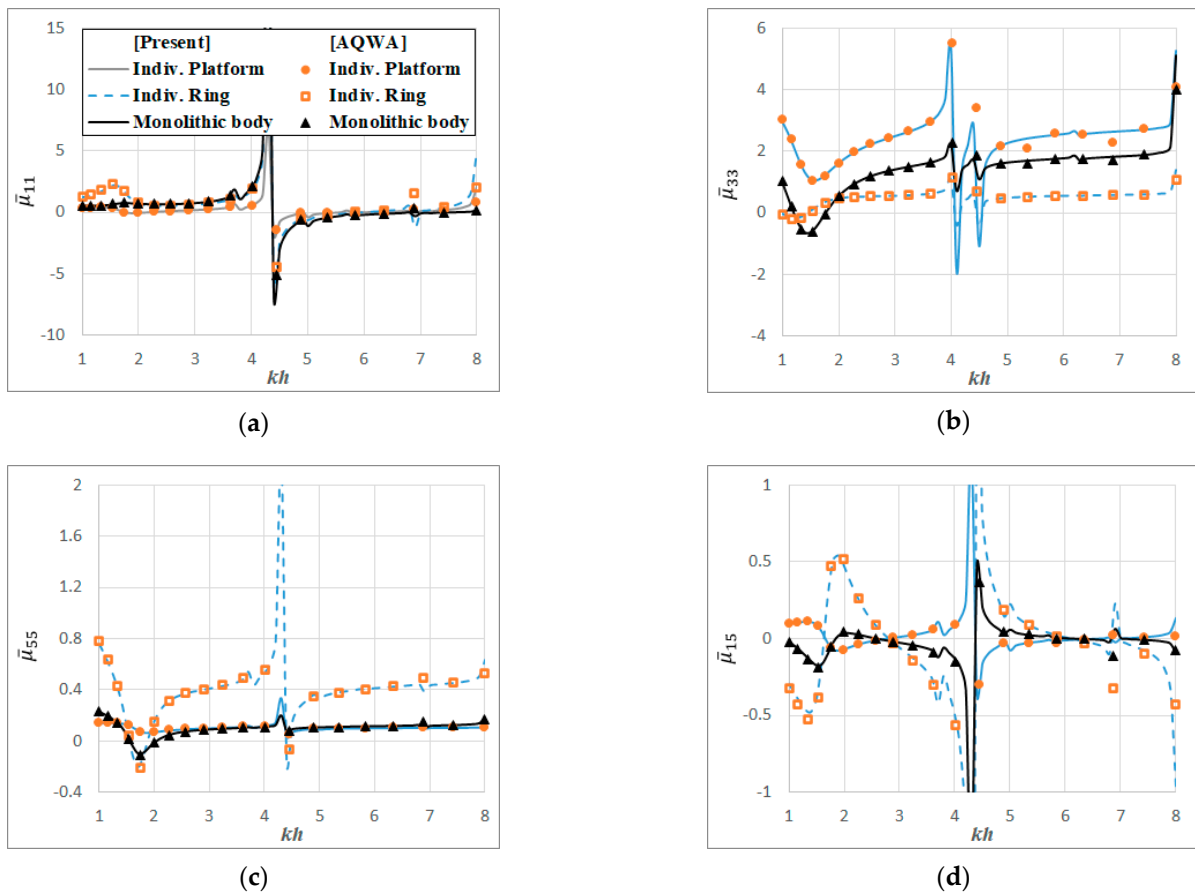


Figure 4. Cont.

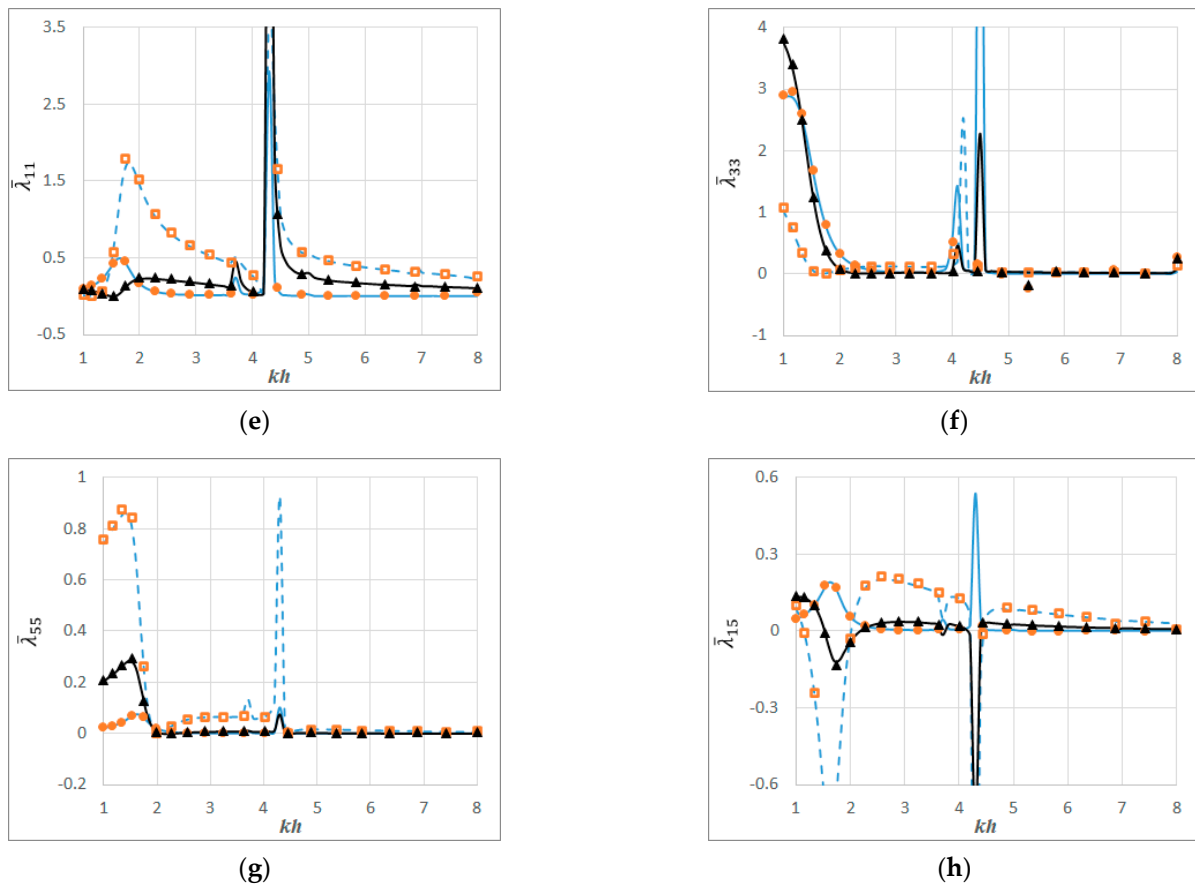


Figure 4. Comparison of normalised added mass and radiation damping obtained from AQWA and present approach: (a) added mass for surge; (b) added mass for heave; (c) added mass for pitch; (d) added mass for surge-pitch; (e) radiation damping for surge; (f) radiation damping for heave; (g) radiation damping for pitch; (h) radiation damping for surge-pitch.

The added mass was normalised by

$$\bar{\mu}_{11}^{(q,p)} = \frac{\mu_{11}^{(q,p)}}{\rho S_{0_q} d_q}; \bar{\mu}_{33}^{(q,p)} = \frac{\mu_{33}^{(q,p)}}{\rho S_{0_q} d_q}; \bar{\mu}_{55}^{(q,p)} = \frac{\mu_{55}^{(q,p)}}{\rho S_{0_q}^2 d_q}; \bar{\mu}_{15}^{(q,p)} = \frac{\mu_{15}^{(q,p)}}{\rho S_{0_q}^{1.5} d_q} \quad (87)$$

while the radiation damping was normalised by

$$\bar{\lambda}_{11}^{(q,p)} = \frac{\lambda_{11}^{(q,p)}}{\rho \omega S_{0_q} d_q}; \bar{\lambda}_{33}^{(q,p)} = \frac{\lambda_{33}^{(q,p)}}{\rho \omega S_{0_q} d_q}; \bar{\lambda}_{55}^{(q,p)} = \frac{\lambda_{55}^{(q,p)}}{\rho \omega S_{0_q}^2 d_q}; \bar{\lambda}_{15}^{(q,p)} = \frac{\lambda_{15}^{(q,p)}}{\rho \omega S_{0_q}^{1.5} d_q} \quad (88)$$

where S_{0_q} is the cross-sectional area of the polygonal platform for $q = 1$ and that of the polygonal ring structure for $q = 2$. The present semi-analytical results and AQWA results are in excellent agreement; thereby confirming the validity, convergence and accuracy of the semi-analytical approach. It can be seen that the magnitudes of crests near resonance frequencies are sensitively varying with minor discrepancies between AQWA and present results (see Figure 4b,d).

The wave exciting forces and RAOs were calculated for $\beta = 0^\circ$. The horizontal wave force, vertical wave force and rotational moment were normalised as follows:

$$\bar{F}_x^{(q)} = \frac{F_x^{(q)}}{\rho g A S_{0_q}}; \bar{F}_z^{(q)} = \frac{F_z^{(q)}}{\rho g A S_{0_q}}; \bar{M}_y^{(q)} = \frac{M_y^{(q)}}{\rho g A S_{0_q} d_q}$$

The RAO (Response Amplitude Operator) is defined as the motion response normalised by the incident wave amplitude A . Figure 5 compares the wave exciting forces and the RAOs obtained from the present semi-analytical method and those computed from ANSYS AQWA. It can be seen that the results are in close agreement; thereby verifying the present semi-analytical formulation and method of solution.

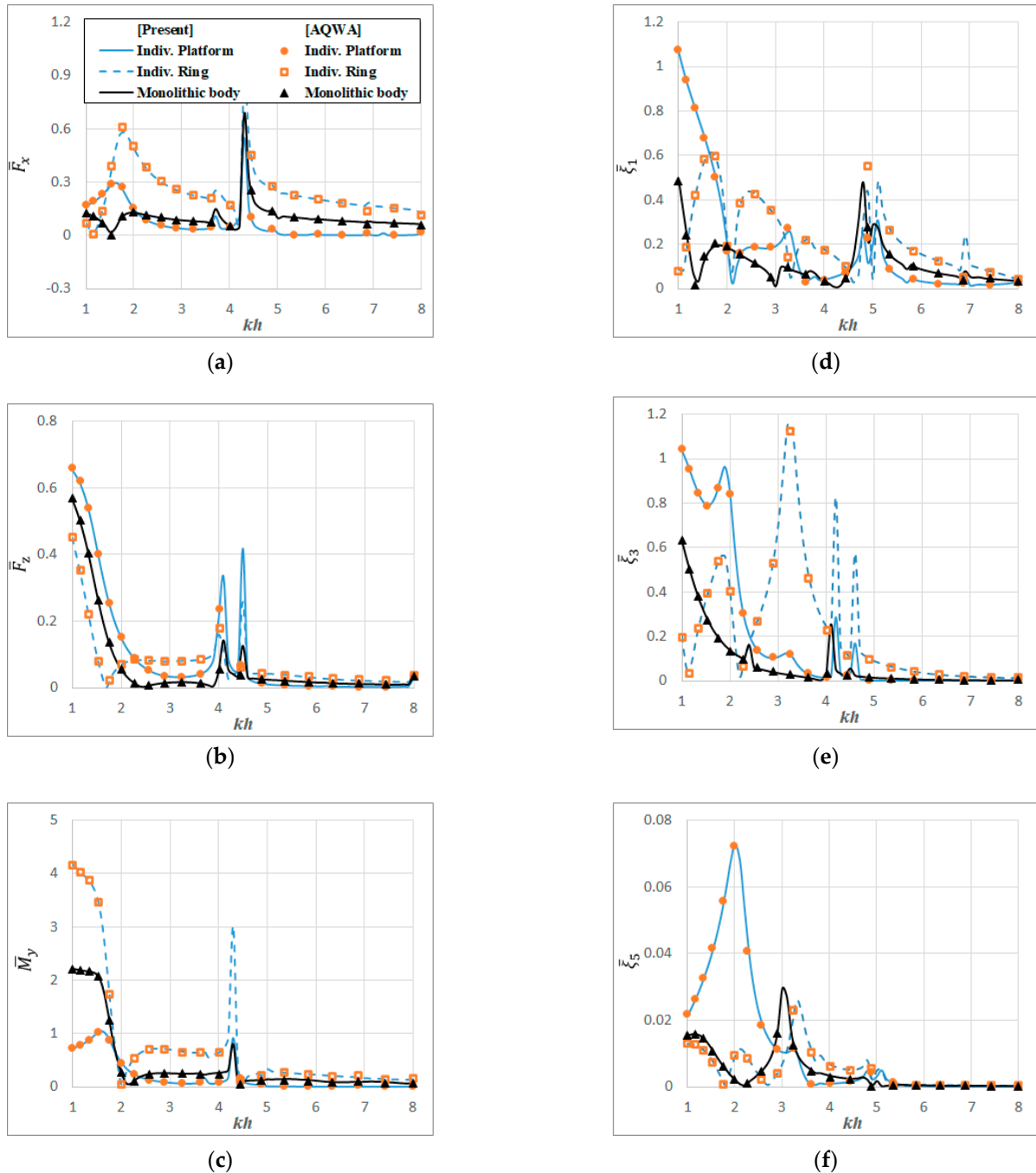


Figure 5. Comparison of wave exciting forces and RAOs obtained from AQWA and present approach: (a) surge force; (b) heave force; (c) pitch moment; (d) RAO for surge; (e) RAO for heave; (f) RAO for pitch.

The wave field and profiles for the inner water basin of the floating hexagonal platform and ring structure were calculated as shown in Figure 6 (for $T = 10$ s). The floating bodies are oscillating together or individually. Wave profiles are drawn along the x -axis at $y = 0$ m

and $y = 50$ m, which are normalised by the incident wave amplitude for the wave period 10 s. The wave profiles obtained from the present approach and AQWA are well matched. Note that the wave profiles belonging to AQWA were extracted from AQWA FLOW by writing a computer code to process the raw data at selected points.

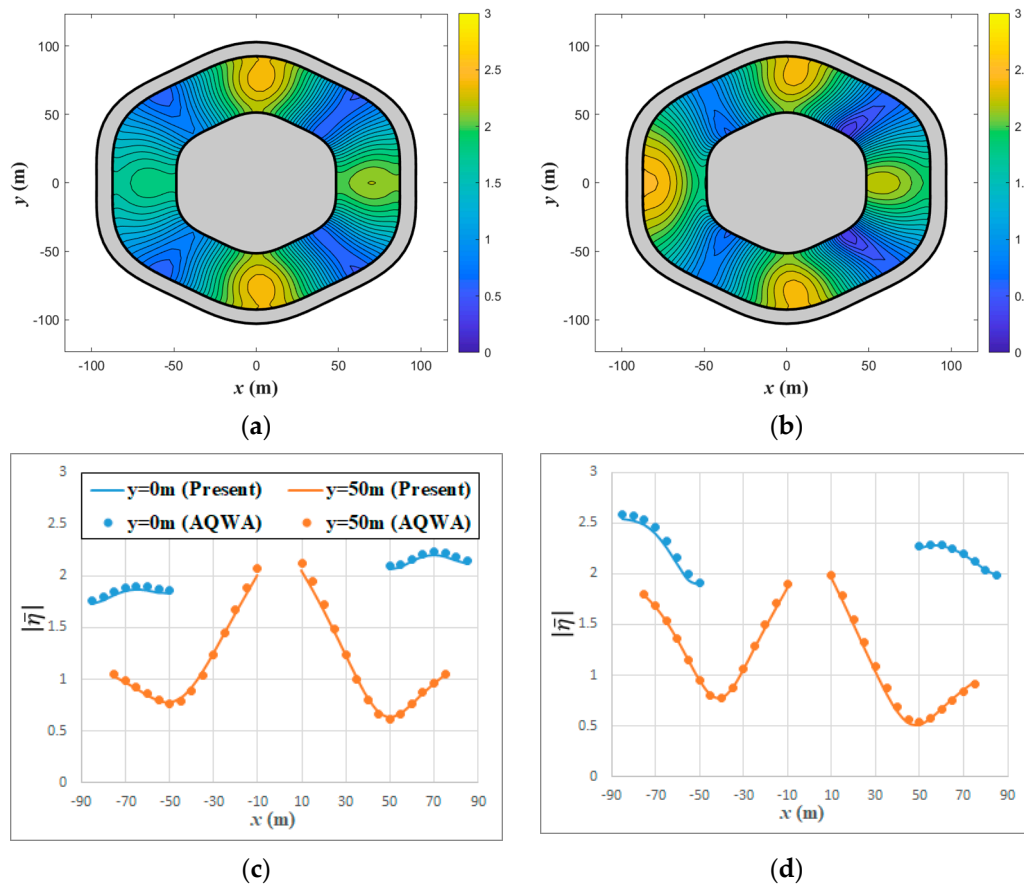


Figure 6. Comparison of normalised wave elevations and profiles for together or individually oscillating floating hexagonal platform and ring structure obtained from AQWA and present approach (for $T = 10$ s): (a) wave field for monolithic motion; (b) wave field for individual motion; (c) wave profile for monolithic motion; (d) wave profile for individual motion.

9. Results and Discussion

Further hydrodynamic analyses have been carried out to investigate various effects due to drafts, the radii of platforms and polygonal shapes. Floating hexagonal platform and ring structure that oscillate individually are considered. The drafts for two individual floating bodies are respectively taken as: (1) $d_1/h = 0.1, d_2/h = 0.1$, (2) $d_1/h = 0.1, d_2/h = 0.2$, (3) $d_1/h = 0.2, d_2/h = 0.1$ and (4) $d_1/h = 0.2, d_2/h = 0.2$. The wave exciting forces and RAOs are given in Figure 7 while the added mass and radiation damping are presented in Figure 8. Note that “P” and “R” used in legends stand for “Platform” and “Ring”, respectively. Overall, the ring structure shows greater dominance in surge and pitch forces while the platform shows dominance in heave forces as shown in Figure 7 as the ring structure primarily prevents wave propagation. For longer waves (say $kh < 2$), as more waves are transmitted into the inner water basin, they become trapped; thereby, creating a high energetic environment within the ring structure. Accordingly, this aggravates the hydrodynamic interaction on the platform. However, the situations are reversed when considering the RAOs for heave and pitch (see Figure 7e,f). Similar phenomena are observed for added mass and radiation damping in the case of heave (see Figure 8b,f). In general, when the ratio of the draft-to-water depth of the ring structure (i.e., d_2/h) is the same, the

hydrodynamic results such as the wave exciting forces, RAOs, added mass and radiation damping associated with the ring structure are very close to each other regardless of the ratio of the draft-to-water depth of the platform (i.e., d_1/h). Likewise, when d_1/h of the platform is the same, the hydrodynamic results associated with the platform are similarly irrelevant to d_2/h .

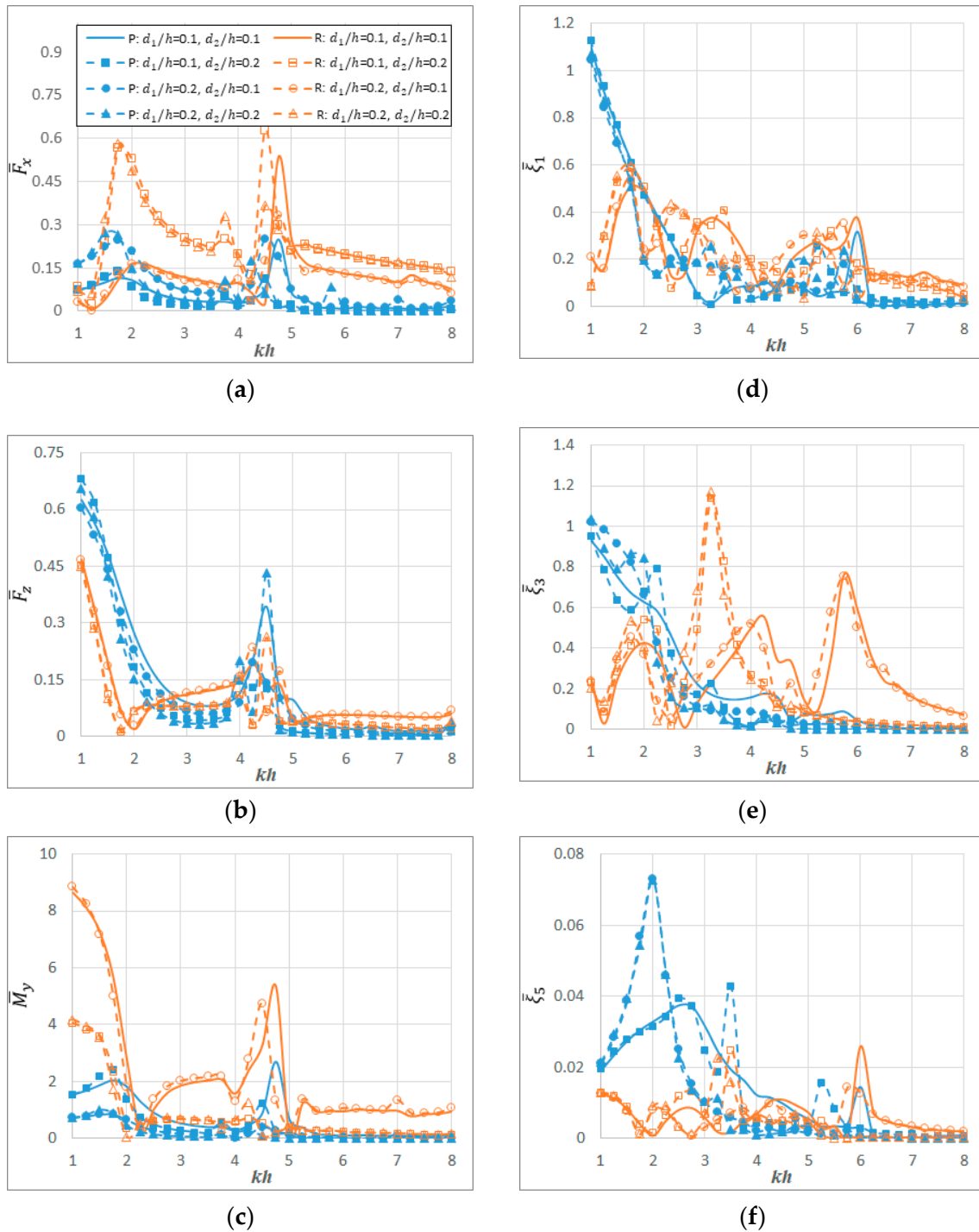


Figure 7. Normalised wave exciting forces and RAOs for floating hexagonal platforms and ring structures with various draft-to-water depth ratios: (a) surge force; (b) heave force; (c) pitch moment; (d) RAO for surge; (e) RAO for heave; (f) RAO for pitch.

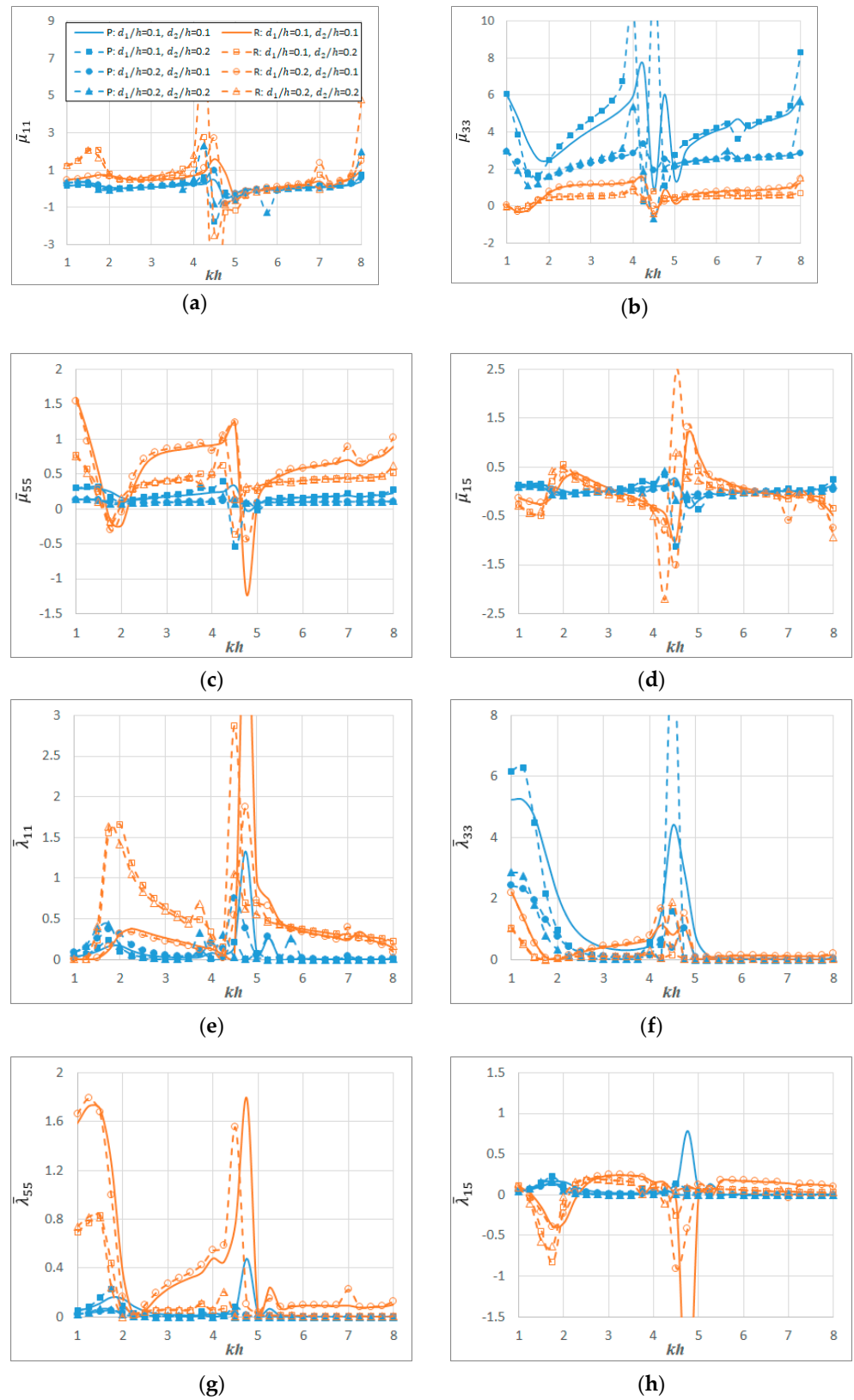


Figure 8. Normalised added mass and radiation damping for floating hexagonal platforms and ring structures with various draft-to-water depth ratios: (a) added mass for surge; (b) added mass for heave; (c) added mass for pitch; (d) added mass for surge-pitch; (e) radiation damping for surge; (f) radiation damping for heave; (g) radiation damping for pitch; (h) radiation damping for surge-pitch.

In Figure 9, the wave exciting forces and RAOs for floating circular platform and ring structure are presented for various radii of the circular platform, i.e., $R_1/h = 0.5, 1, 1.5$. It can be seen that the wave exciting forces increase with increasing R_1/h . On the other hand, the RAOs for the platform decrease with increasing R_1/h , whereas the RAOs for the ring structure do not show a distinctive relationship. This implies that a large working platform placed within a floating ring breakwater is relatively stable in terms of motions when compared with a small platform. On the other hand, when a small oscillating cylindrical platform is deployed within a floating ring structure, relatively large kinetic energy can be obtained.

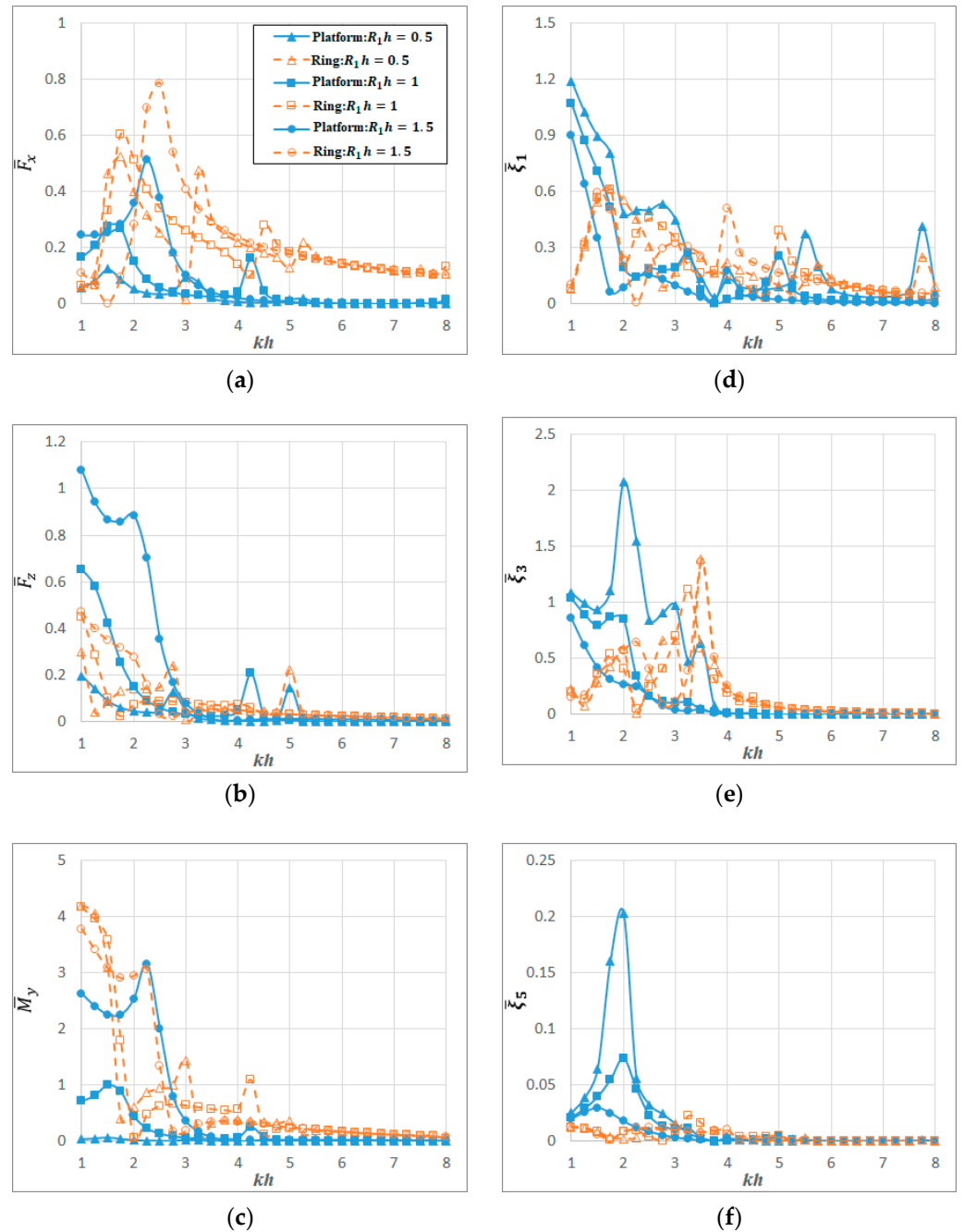


Figure 9. Normalised wave exciting forces and RAOs for floating circular platform and circular ring structure with $R_1/h = 0.5, 1, 1.5$: (a) surge force; (b) heave force; (c) pitch moment; (d) RAO for surge; (e) RAO for heave; (f) RAO for pitch.

Next, the free water surface elevation in the inner water basin will be investigated for the various geometries of floating polygonal platform and ring structure. Added mass, radiation damping and RAOs do not represent significant differences for similar sizes of plan shapes as when their geometries are created by using the radius function as given in Equation (1), the plan shapes for every kind of polygons are almost the same as each other. In addition, as far as the wave exciting forces are concerned, the horizontal forces such as surge or sway forces are distinctively changed when polygonal shapes are appropriately used with their orientations. This phenomenon was already reported by Park and Wang [20]. Hence, in this parametric study, the free water surface elevation in the inner water basin will be the focus.

The floating circular platform and circular ring structure are initially considered to investigate the inner wave fields. The draft-to-water depth ratio for the circular floating bodies $d_1/h = 0.1, 0.2$ and $d_2/h = 0.1, 0.2$ are combined into 4 cases. The inner wave fields at significant resonance frequencies are presented in Figure 10 by assuming the water depth $h = 50$ m. The maximum value of the scale bar is set to 4; implying wave fields larger than 4 are included in the maximum value (yellow colour). It can be learned that when larger d_2 and smaller d_1 are considered, there will be more waves trapped in the inner water basin, resulting in higher free water surface elevation (see Figure 10b) and vice versa. Thus, Figure 10b may be used for harvesting more wave energy, whereas Figure 10c is used for creating a calm patch of water space.

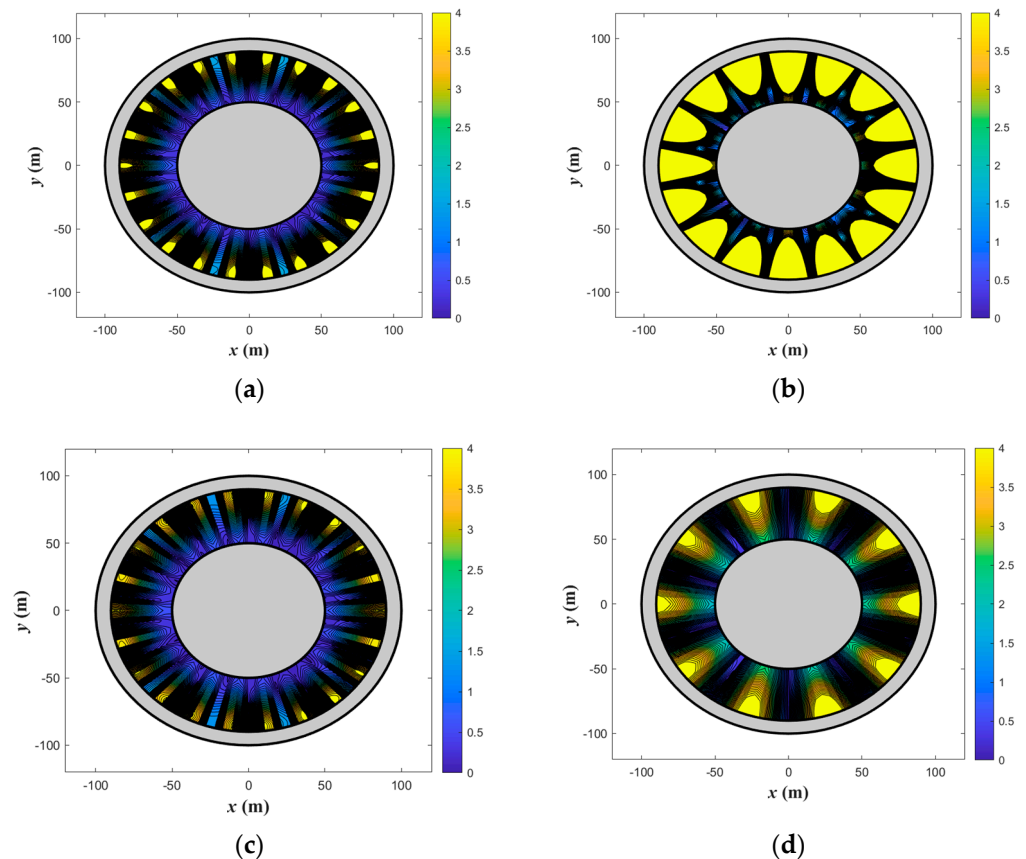


Figure 10. Normalised inner wave fields for individually oscillating floating circular platforms and ring structures at significant resonance frequencies: (a) $d_1/h = 0.1, d_2/h = 0.1$ ($kh = 7.5$); (b) $d_1/h = 0.1, d_2/h = 0.2$ ($kh = 5.5$); (c) $d_1/h = 0.2, d_2/h = 0.1$ ($kh = 7.5$); (d) $d_1/h = 0.2, d_2/h = 0.2$ ($kh = 3.75$).

In order to investigate the shape effect on the inner wave fields, several combinations of different polygonal shapes such as a square, hexagon and circle are considered for

$d_1/h = d_2/h = 0.2$ by assuming the water depth $h = 50$ m. Normalised inner wave fields for various floating polygonal platforms and ring structures at significant resonance frequencies are presented in Figure 11. By referring to Figure 10d together with Figure 11, it can be found that the inner wave fields at the significant resonance frequency for circular shapes tend to spread waves to multiple directions (see Figure 10d). For the square shapes, the inner wave fields are mild when compared with other cases (see Figure 11a) and amplified waves appeared to be in one direction (see Figure 11c,e). For the hexagonal shapes, waves are more amplified than the circular shapes and their propagations are in multiple directions. This implies that the square shapes are beneficial in terms of creating a calm patch of water space, whereas the hexagonal shapes are more advantageous for wave energy harvesting.

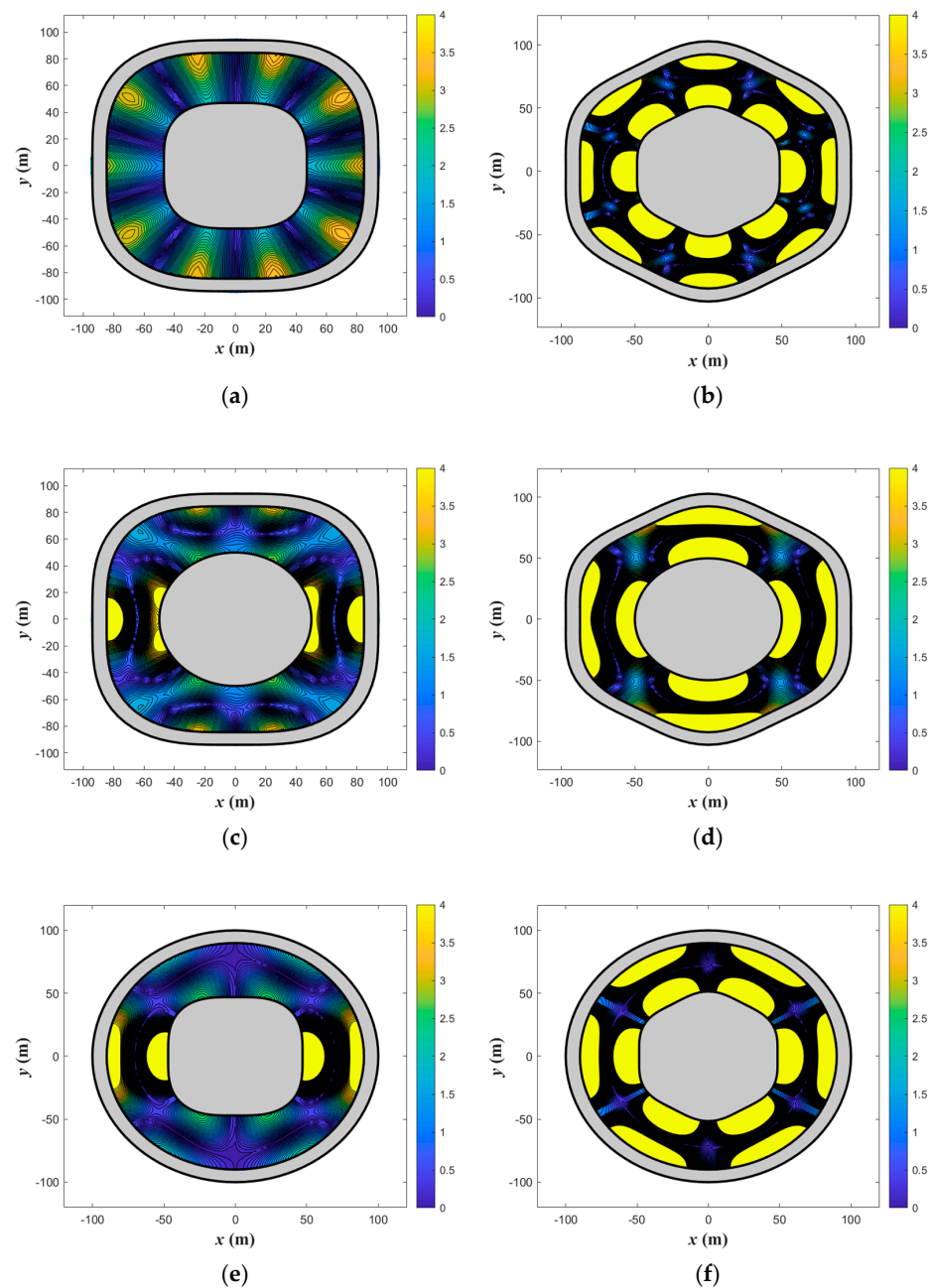


Figure 11. Normalised inner wave fields for various combinations of individually oscillating floating

platforms and ring structures at significant resonance frequencies: (a) square platform and square ring ($kh = 3.75$); (b) hexagonal platform and hexagonal ring ($kh = 5.25$); (c) circular platform and square ring ($kh = 5.25$); (d) circular platform and hexagonal ring ($kh = 4.5$); (e) square platform and circular ring ($kh = 4.75$); (f) hexagonal platform and circular ring ($kh = 4.75$).

10. Concluding Remarks

A semi-analytical method and computer code have been developed for the hydrodynamic analysis of a floating regular polygonal platform that is centrally placed within a regular polygonal ring structure under wave action. The polygonal shapes for equilateral triangle, square, pentagonal, hexagonal platforms and ring structures can be readily generated by using the cosine-type radial perturbation. This shape function is the key to enabling the problem to be solved semi-analytically. Cases involving the two floating bodies oscillating together or individually were considered with the view to understanding the hydrodynamic interactions among the trapped waves, inner platform and outer ring structure. The method has been shown to be able to furnish accurate hydrodynamic quantities such as wave exciting forces, added mass, radiation damping, RAOs, and wave field. The computational speed has been significantly quickened when compared with numerical methods because of the semi-analytical method.

The effects of several parameters such as drafts, radii of platforms and polygonal shapes on major hydrodynamic quantities are investigated by performing parametric studies. When the draft of the ring structure is larger than the floating platform, trapped waves are amplified more in the inner water basin. Additionally, the wave exciting forces increase with increasing radii of platforms. However, the RAOs decrease with the increasing radii of platforms. The inner wave fields for circular shapes tend to spread waves to multiple directions, whereas those for square shapes are relatively mild and their amplified waves are apt to propagate in one direction. For hexagonal shapes, the wave fields are more amplified than other considered shapes and the waves' propagations are in multiple directions. In sum, floating square platform and square ring structure are beneficial for creating a calm patch of water space, whereas the floating hexagonal platform and the hexagonal ring structure are more advantageous for wave energy harvesting.

Author Contributions: Conceptualization, J.C.P. and C.M.W.; methodology, J.C.P.; software, J.C.P.; validation, J.C.P. and C.M.W.; formal analysis, J.C.P.; investigation, J.C.P. and C.M.W.; writing—original draft preparation, J.C.P.; writing—review and editing, C.M.W.; visualization, J.C.P.; supervision, C.M.W.; funding acquisition, C.M.W.; All authors have read and agreed to the published version of the manuscript.

Funding: This research was supported by the Australian Government through the Australian Research Council's Discovery Projects funding scheme (project DP170104546). The views expressed herein are those of the authors and are not necessarily those of the Australian Government or Australian Research Council.

Institutional Review Board Statement: Not applicable.

Informed Consent Statement: Not applicable.

Data Availability Statement: Not applicable.

Conflicts of Interest: The authors declare no conflict of interest.

Appendix A

The divergences between the generalised motion normal \mathbf{n}_j and unit normal vector \mathbf{n}_{s_l} ($l = 1, 2, 3$) at $r = R_l(\theta)$ are calculated for 6 DOFs in the Cartesian coordinate system as given by

$$\mathbf{n}_1 \cdot \mathbf{n}_{s_l} = \mathbf{n}_x \cdot \mathbf{n}_{s_l} = \frac{\cos \theta - \frac{\sin \theta}{R_l} S_{l,\theta}}{\sqrt{1 + \frac{S_{l,\theta}^2}{R_l^2}}} \tag{A1}$$

$$\mathbf{n}_2 \cdot \mathbf{n}_{s_l} = \mathbf{n}_y \cdot \mathbf{n}_{s_l} = \frac{\sin \theta + \frac{\cos \theta}{R_l} S_{l,\theta}}{\sqrt{1 + \frac{S_{l,\theta}^2}{R_l^2}}} \tag{A2}$$

$$\mathbf{n}_3 \cdot \mathbf{n}_{s_l} = \mathbf{n}_z \cdot \mathbf{n}_{s_l} = 0 \tag{A3}$$

$$\mathbf{n}_4 \cdot \mathbf{n}_s = -(z - z_G) \mathbf{n}_y \cdot \mathbf{n}_{s_l} + (y - y_G) \mathbf{n}_z \cdot \mathbf{n}_{s_l} = -\frac{(z - z_G) \left(\sin \theta + \frac{\cos \theta}{R_l} S_{l,\theta} \right)}{\sqrt{1 + \frac{S_{l,\theta}^2}{R_l^2}}} \tag{A4}$$

$$\mathbf{n}_5 \cdot \mathbf{n}_s = (z - z_G) \mathbf{n}_x \cdot \mathbf{n}_{s_l} - (x - x_G) \mathbf{n}_z \cdot \mathbf{n}_{s_l} = \frac{(z - z_G) \left(\cos \theta - \frac{\sin \theta}{R_l} S_{l,\theta} \right)}{\sqrt{1 + \frac{S_{l,\theta}^2}{R_l^2}}} \tag{A5}$$

$$\mathbf{n}_6 \cdot \mathbf{n}_{s_l} = -(y - y_G) \mathbf{n}_x \cdot \mathbf{n}_{s_l} + (x - x_G) \mathbf{n}_y \cdot \mathbf{n}_{s_l} = \frac{S_{l,\theta} + (y_G - x_G) \left(\cos \theta + \sin \theta - \frac{\sin \theta - \cos \theta}{R_l} S_{l,\theta} \right)}{\sqrt{1 + \frac{S_{l,\theta}^2}{R_l^2}}} \tag{A6}$$

If $S_{l,\theta} = 0$, it can be applied to a circular platform or ring breakwater.

Appendix B

The reduced expressions $H_l^{(j)}$, $P_l^{(j)}$, $Q_l^{(j)}$, $\tilde{P}_l^{(j)}$ and $\tilde{Q}_l^{(j)}$ ($j = 0, 1, \dots, 6; l = 1, 2, 3$) introduced in Equations (31)–(39) and Equations (50)–(58) are given by

$$\begin{aligned} H_l^{(0)} &= \frac{igA}{\omega \cosh kh} \sum_{m=-\infty}^{\infty} e^{im(\frac{\pi}{2}-\beta)} \mathcal{J}'_{m0}(kR_l) e^{im\theta} \cosh k(z+h) \\ &= \frac{igA}{\omega \cosh kh} \sum_{m=-\infty}^{\infty} e^{im(\frac{\pi}{2}-\beta)} \sum_{q=-\infty}^{\infty} \sum_{n_r=-\infty}^{\infty} \left[\frac{k}{2} b_{2,0,n_r}^{(l)} \{ f_{m-1,q}^{(l)} - f_{m+1,q}^{(l)} \} + mn_r b_{1,0,n_r}^{(l)} f_{m,q}^{(l)} \right] e^{i(m+q+n_r)\theta} \cosh k(z+h) \end{aligned} \tag{A7}$$

$$H_l^{(1)} = R_l^2 \cos \theta - R_l S_{l,\theta} \sin \theta = \frac{1}{4} \sum_{n_r=-\infty}^{\infty} \left\{ (n_r + 1) b_{2,0,n_r-1}^{(l)} - (n_r - 1) b_{2,0,n_r+1}^{(l)} \right\} e^{in_r\theta} \tag{A8}$$

$$H_l^{(2)} = R_l^2 \sin \theta + R_l S_{l,\theta} \cos \theta = \frac{1}{4i} \sum_{n_r=-\infty}^{\infty} \left\{ (n_r + 1) b_{2,0,n_r-1}^{(l)} + (n_r - 1) b_{2,0,n_r+1}^{(l)} \right\} e^{in_r\theta} \tag{A9}$$

$$H_l^{(3)} = 0 \tag{A10}$$

$$\begin{aligned} H_l^{(4)} &= -(z - z_{G_p}) \left(R_l^2 \sin \theta + R_l S_{l,\theta} \cos \theta \right) \\ &= -\frac{(z - z_{G_p})}{4i} \sum_{n_r=-\infty}^{\infty} \left\{ (n_r + 1) b_{2,0,n_r-1}^{(l)} + (n_r - 1) b_{2,0,n_r+1}^{(l)} \right\} e^{in_r\theta} \end{aligned} \tag{A11}$$

$$\begin{aligned} H_l^{(5)} &= (z - z_{G_p}) \left(R_l^2 \cos \theta - R_l S_{l,\theta} \sin \theta \right) \\ &= \frac{(z - z_{G_p})}{4} \sum_{n_r=-\infty}^{\infty} \left\{ (n_r + 1) b_{2,0,n_r-1}^{(l)} - (n_r - 1) b_{2,0,n_r+1}^{(l)} \right\} e^{in_r\theta} \end{aligned} \tag{A12}$$

$$H_l^{(6)} = R_l^2 S_{l,\theta} = -\frac{in_r}{3} \sum_{n_r=-\infty}^{\infty} b_{3,0,n_r}^{(l)} e^{in_r\theta} \tag{A13}$$

where $S_{l,\theta}$ denotes $\left. \frac{\partial S_l}{\partial \theta} \right|_{r=R_l(\theta)}$ and z_{G_p} the z-coordinate of the centre of gravity for the oscillating body p .

$$\begin{aligned} \tilde{P}_l^{(0)} &= \frac{igA}{\omega \cosh kh} \sum_{m=-\infty}^{\infty} e^{im(\frac{\pi}{2}-\beta)} \mathcal{J}'_{m0}(kR_l) e^{im\theta} \cosh k(z+h) \\ &= \frac{igA}{\omega \cosh kh} \sum_{m=-\infty}^{\infty} e^{im(\frac{\pi}{2}-\beta)} \sum_{q=-\infty}^{\infty} \sum_{n_r=-\infty}^{\infty} \left[\frac{k}{2} b_{2,0,n_r}^{(l)} \{ f_{m-1,q}^{(l)} - f_{m+1,q}^{(l)} \} + mn_r b_{1,0,n_r}^{(l)} f_{m,q}^{(l)} \right] e^{i(m+q+n_r)\theta} \cosh k(z+h) \end{aligned} \tag{A14}$$

$$\tilde{P}_l^{(3)} = -\frac{R_l^3}{2(h - d_1)} = -\frac{1}{2(h - d_1)} \sum_{n_r=-\infty}^{\infty} b_{3,0,n_r}^{(l)} e^{in_r\theta} \tag{A15}$$

$$\begin{aligned} \tilde{P}_l^{(4)} &= \frac{1}{8(h-d_1)} \left\{ 4(z+h)^2 (R_l^2 \sin \theta + R_l S_{l,\theta} \cos \theta) - (3R_l^4 \sin \theta + R_l^3 \cos \theta S_{l,\theta}) \right\} \\ &= -\frac{i}{64(h-d_1)} \sum_{n_r=-\infty}^{\infty} \left[8(z+h)^2 \left\{ (n_r+1)b_{2,0,n_r-1}^{(l)} + (n_r-1)b_{2,0,n_r+1}^{(l)} \right\} \right. \\ &\quad \left. - \left\{ (n_r+11)b_{4,0,n_r-1}^{(l)} + (n_r-11)b_{4,0,n_r+1}^{(l)} \right\} \right] e^{in_r\theta} \end{aligned} \tag{A16}$$

$$\begin{aligned} \tilde{P}_l^{(5)} &= -\frac{1}{8(h-d_1)} \left\{ 4(z+h)^2 (R_l^2 \cos \theta - R_l S_{l,\theta} \sin \theta) - (3R_l^4 \cos \theta - R_l^3 \sin \theta S_{l,\theta}) \right\} \\ &= -\frac{1}{64(h-d_1)} \sum_{n_r=-\infty}^{\infty} \left[8(z+h)^2 \left\{ (n_r+1)b_{2,0,n_r-1}^{(l)} - (n_r-1)b_{2,0,n_r+1}^{(l)} \right\} \right. \\ &\quad \left. - \left\{ (n_r+11)b_{4,0,n_r-1}^{(l)} - (n_r-11)b_{4,0,n_r+1}^{(l)} \right\} \right] e^{in_r\theta} \end{aligned} \tag{A17}$$

$$\tilde{P}_l^{(1)} = \tilde{P}_l^{(2)} = \tilde{P}_l^{(6)} = 0 \tag{A18}$$

$$\begin{aligned} P_l^{(0)} &= \frac{igA}{\omega \cosh kh} \sum_{m=-\infty}^{\infty} e^{im(\frac{\pi}{2}-\beta)} J_m(kR_l) e^{im\theta} \cosh k(z+h) \\ &= \frac{igA}{\omega \cosh kh} \sum_{m=-\infty}^{\infty} e^{im(\frac{\pi}{2}-\beta)} \sum_{q=-\infty}^{\infty} f_{m,q}^{(l)} e^{i(m+q)\theta} \cosh k(z+h) \end{aligned} \tag{A19}$$

$$P_l^{(3)} = \frac{2(z+h)^2 - R_l^2}{4(h-d_1)} = \frac{(z+h)^2}{2(h-d)} - \frac{1}{4(h-d)} \sum_{n_r=-\infty}^{\infty} b_{2,0,n_r}^{(l)} e^{in_r\theta} \tag{A20}$$

$$\begin{aligned} P_l^{(4)} &= \frac{4(z+h)^2 - R_l^2}{8(h-d_1)} R_l \sin \theta \\ &= -\frac{i}{16(h-d_1)} \sum_{n_r=-\infty}^{\infty} \left[4(z+h)^2 \left\{ b_{1,0,n_r-1}^{(l)} - b_{1,0,n_r+1}^{(l)} \right\} - \left\{ b_{3,0,n_r-1}^{(l)} - b_{3,0,n_r+1}^{(l)} \right\} \right] e^{in_r\theta} \end{aligned} \tag{A21}$$

$$\begin{aligned} P_l^{(5)} &= -\frac{4(z+h)^2 - R_l^2}{8(h-d_1)} R_l \cos \theta \\ &= -\frac{1}{16(h-d_1)} \sum_{n_r=-\infty}^{\infty} \left[4(z+h)^2 \left\{ b_{1,0,n_r-1}^{(l)} + b_{1,0,n_r+1}^{(l)} \right\} - \left\{ b_{3,0,n_r-1}^{(l)} + b_{3,0,n_r+1}^{(l)} \right\} \right] e^{in_r\theta} \end{aligned} \tag{A22}$$

$$P_l^{(1)} = P_l^{(2)} = P_l^{(6)} = 0 \tag{A23}$$

$$\begin{aligned} \tilde{Q}_l^{(0)} &= \frac{igA}{\omega \cosh kh} \sum_{m=-\infty}^{\infty} e^{im(\frac{\pi}{2}-\beta)} \mathcal{J}_{m0}^l(kR_l) e^{im\theta} \cosh k(z+h) \\ &= \frac{igA}{\omega \cosh kh} \sum_{m=-\infty}^{\infty} e^{im(\frac{\pi}{2}-\beta)} \sum_{q=-\infty}^{\infty} \sum_{n_r=-\infty}^{\infty} \left[\frac{k}{2} b_{2,0,n_r}^{(l)} \left\{ f_{m-1,q}^{(l)} - f_{m+1,q}^{(l)} \right\} + mn_r b_{1,0,n_r}^{(l)} f_{m,q}^{(l)} \right] e^{i(m+q+n_r)\theta} \cosh k(z+h) \end{aligned} \tag{A24}$$

$$\tilde{Q}_l^{(3)} = -\frac{R_l^3}{2(h-d_2)} = -\frac{1}{2(h-d_2)} \sum_{n_r=-\infty}^{\infty} b_{3,0,n_r}^{(l)} e^{in_r\theta} \tag{A25}$$

$$\begin{aligned} \tilde{Q}_l^{(4)} &= \frac{1}{8(h-d_2)} \left\{ 4(z+h)^2 (R_l^2 \sin \theta + R_l S_{l,\theta} \cos \theta) - (3R_l^4 \sin \theta + R_l^3 \cos \theta S_{l,\theta}) \right\} \\ &= -\frac{i}{64(h-d_2)} \sum_{n_r=-\infty}^{\infty} \left[8(z+h)^2 \left\{ (n_r+1)b_{2,0,n_r-1}^{(l)} + (n_r-1)b_{2,0,n_r+1}^{(l)} \right\} - \left\{ (n_r+11)b_{4,0,n_r-1}^{(l)} + (n_r-11)b_{4,0,n_r+1}^{(l)} \right\} \right] e^{in_r\theta} \end{aligned} \tag{A26}$$

$$\begin{aligned} \tilde{Q}_l^{(5)} &= -\frac{1}{8(h-d_2)} \left\{ 4(z+h)^2 (R_l^2 \cos \theta - R_l S_{l,\theta} \sin \theta) - (3R_l^4 \cos \theta - R_l^3 \sin \theta S_{l,\theta}) \right\} \\ &= -\frac{1}{64(h-d_2)} \sum_{n_r=-\infty}^{\infty} \left[8(z+h)^2 \left\{ (n_r+1)b_{2,0,n_r-1}^{(l)} - (n_r-1)b_{2,0,n_r+1}^{(l)} \right\} \right. \\ &\quad \left. - \left\{ (n_r+11)b_{4,0,n_r-1}^{(l)} - (n_r-11)b_{4,0,n_r+1}^{(l)} \right\} \right] e^{in_r\theta} \end{aligned} \tag{A27}$$

$$\tilde{Q}_l^{(1)} = \tilde{Q}_l^{(2)} = \tilde{Q}_l^{(6)} = 0 \tag{A28}$$

$$\begin{aligned} Q_l^{(0)} &= \frac{igA}{\omega \cosh kh} \sum_{m=-\infty}^{\infty} e^{im(\frac{\pi}{2}-\beta)} J_m(kR_l) e^{im\theta} \cosh k(z+h) \\ &= \frac{igA}{\omega \cosh kh} \sum_{m=-\infty}^{\infty} e^{im(\frac{\pi}{2}-\beta)} \sum_{q=-\infty}^{\infty} f_{m,q}^{(l)} e^{i(m+q)\theta} \cosh k(z+h) \end{aligned} \tag{A29}$$

$$Q_l^{(3)} = \frac{2(z+h)^2 - R_l^2}{4(h-d_2)} = \frac{(z+h)^2}{2(h-d_2)} - \frac{1}{4(h-d_2)} \sum_{n_r=-\infty}^{\infty} b_{2,0,n_r}^{(l)} e^{in_r\theta} \tag{A30}$$

$$Q_i^{(4)} = \frac{4(z+h)^2 - R_i^2}{8(h-d_2)} R_i \sin \theta$$

$$= -\frac{i}{16(h-d_2)} \sum_{n_r=-\infty}^{\infty} \left[4(z+h)^2 \{ b_{1,0,n_r-1}^{(l)} - b_{1,0,n_r+1}^{(l)} \} - \{ b_{3,0,n_r-1}^{(l)} - b_{3,0,n_r+1}^{(l)} \} \right] e^{in_r \theta} \tag{A31}$$

$$Q_i^{(5)} = -\frac{4(z+h)^2 - R_i^2}{8(h-d_2)} R_i \cos \theta$$

$$= -\frac{1}{16(h-d_2)} \sum_{n_r=-\infty}^{\infty} \left[4(z+h)^2 \{ b_{1,0,n_r-1}^{(l)} + b_{1,0,n_r+1}^{(l)} \} - \{ b_{3,0,n_r-1}^{(l)} + b_{3,0,n_r+1}^{(l)} \} \right] e^{in_r \theta} \tag{A32}$$

$$Q_i^{(1)} = Q_i^{(2)} = Q_i^{(6)} = 0 \tag{A33}$$

Appendix C

The reduced expressions $\tilde{a}_{m,n,q}^{(1)}$, $\tilde{b}_{m,n,q}^{(1),(2)}$, $\tilde{c}_{m,n,q}^{(1),(2)}$, $\tilde{d}_{m,n,q}^{(2),(3)}$, $\tilde{e}_{m,n,q}^{(2),(3)}$, $\tilde{f}_{m,n,q}^{(3)}$, $\tilde{a}'_{m,n,q}^{(1)}$, $\tilde{b}'_{m,n,q}^{(1),(2)}$, $\tilde{c}'_{m,n,q}^{(1),(2)}$, $\tilde{d}'_{m,n,q}^{(2),(3)}$ and $\tilde{f}'_{m,n,q}^{(3)}$ introduced in Equations (50)–(58) are given by

$$\tilde{a}_{m,0,q}^{(1)} = \frac{a_{m,0,q}^{(1)}}{b_1^{|m|}} (n = 0), \quad \tilde{a}_{m,n,q}^{(1)} = \frac{a_{m,n,q}^{(1)}}{I_m(p_n b_1)} (n > 0) \tag{A34}$$

$$\tilde{a}'_{m,0,q}^{(1)} = \frac{1}{b_1^{|m|}} \left(|m| a_{1,0,n_r}^{(1)} a_{m,0,q}^{(1)} + mn_r a_{1,0,n_r}^{(1)} a_{m,0,q}^{(1)} \right) (n = 0) \tag{A35}$$

$$\tilde{a}'_{m,n,q}^{(1)} = \frac{1}{I_m(p_n b_1)} \left\{ \frac{p_n}{2} a_{2,0,n_r}^{(1)} \left(a_{m-1,n,q}^{(1)} + a_{m+1,n,q}^{(1)} \right) + mn_r a_{1,0,n_r}^{(1)} a_{m,n,q}^{(1)} \right\} (n > 0) \tag{A36}$$

$$\tilde{b}_{m,0,q}^{(1,2)} = b_{m,0,q}^{(1,2)} (n = 0), \quad \tilde{b}_{m,n,q}^{(1,2)} = \frac{b_{m,n,q}^{(1,2)}}{I_m(k_n b_2)} (n > 0) \tag{A37}$$

$$\tilde{b}'_{m,0,q}^{(1)} = \frac{k}{2} a_{2,0,n_r}^{(1)} \left(b_{m-1,0,q}^{(1)} - b_{m+1,0,q}^{(1)} \right) + mn_r a_{1,0,n_r}^{(1)} b_{m,0,q}^{(1)} (n = 0) \tag{A38}$$

$$\tilde{b}'_{m,0,q}^{(2)} = \frac{k}{2} a_{2,0,n_r}^{(2)} \left(b_{m-1,0,q}^{(2)} - b_{m+1,0,q}^{(2)} \right) + mn_r a_{1,0,n_r}^{(2)} b_{m,0,q}^{(2)} (n = 0) \tag{A39}$$

$$\tilde{b}'_{m,n,q}^{(1)} = \frac{1}{I_m(k_n b_2)} \left\{ \frac{k_n}{2} a_{2,0,n_r}^{(1)} \left(b_{m-1,n,q}^{(1)} + b_{m+1,n,q}^{(1)} \right) + mn_r a_{1,0,n_r}^{(1)} b_{m,n,q}^{(1)} \right\} (n > 0) \tag{A40}$$

$$\tilde{b}'_{m,n,q}^{(2)} = \frac{1}{I_m(k_n b_2)} \left\{ \frac{k_n}{2} a_{2,0,n_r}^{(2)} \left(b_{m-1,n,q}^{(2)} + b_{m+1,n,q}^{(2)} \right) + mn_r a_{1,0,n_r}^{(2)} b_{m,n,q}^{(2)} \right\} (n > 0) \tag{A41}$$

$$\tilde{c}_{m,0,q}^{(1,2)} = \frac{c_{m,0,q}^{(1,2)}}{H_m(k a_1)} (n = 0), \quad \tilde{c}_{m,n,q}^{(1,2)} = \frac{c_{m,n,q}^{(1,2)}}{K_m(k_n a_1)} (n > 0) \tag{A42}$$

$$\tilde{c}'_{m,0,q}^{(1)} = \frac{1}{H_m(k a_1)} \left\{ \frac{k}{2} a_{2,0,n_r}^{(1)} \left(c_{m-1,0,q}^{(1)} - c_{m+1,0,q}^{(1)} \right) + mn_r a_{1,0,n_r}^{(1)} c_{m,0,q}^{(1)} \right\} (n = 0) \tag{A43}$$

$$\tilde{c}'_{m,0,q}^{(2)} = \frac{1}{H_m(k a_1)} \left\{ \frac{k}{2} a_{2,0,n_r}^{(2)} \left(c_{m-1,0,q}^{(2)} - c_{m+1,0,q}^{(2)} \right) + mn_r a_{1,0,n_r}^{(2)} c_{m,0,q}^{(2)} \right\} (n = 0) \tag{A44}$$

$$\tilde{c}'_{m,n,q}^{(1)} = \frac{1}{K_m(k_n a_1)} \left\{ -\frac{k_n}{2} a_{2,0,n_r}^{(1)} \left(c_{m-1,n,q}^{(1)} + c_{m+1,n,q}^{(1)} \right) + mn_r a_{1,0,n_r}^{(1)} c_{m,n,q}^{(1)} \right\} (n > 0) \tag{A45}$$

$$\tilde{c}'_{m,n,q}^{(2)} = \frac{1}{K_m(k_n a_1)} \left\{ -\frac{k_n}{2} a_{2,0,n_r}^{(2)} \left(c_{m-1,n,q}^{(2)} + c_{m+1,n,q}^{(2)} \right) + mn_r a_{1,0,n_r}^{(2)} c_{m,n,q}^{(2)} \right\} (n > 0) \tag{A46}$$

$$\tilde{d}_{0,0,q}^{(2,3)} = d_{0,0,q}^{(2,3)} (m = 0, n = 0), \quad \tilde{d}_{m,0,q}^{(2,3)} = \frac{d_{m,0,q}^{(2,3)}}{b_3^{|m|}} (m \neq 0, n = 0) \tag{A47}$$

$$\tilde{d}_{m,n,q}^{(2,3)} = \frac{d_{m,n,q}^{(2,3)}}{I_m(q_n b_3)} \quad (n > 0) \tag{A48}$$

$$\tilde{d}'_{0,0,q}^{(2,3)} = d_{2,0,n_r}^{(2,3)} e_{1,0,q}^{(2,3)} \quad (m = 0, n = 0) \tag{A49}$$

$$\tilde{d}'_{m,0,q}^{(2,3)} = \frac{1}{b_3^{|m|}} \left\{ |m| d_{1,0,n_r}^{(2,3)} d_{m,0,q}^{(2,3)} + mn_r d_{1,0,n_r}^{(2,3)} d_{m,0,q}^{(2,3)} \right\} \quad (m \neq 0, n = 0) \tag{A50}$$

$$\tilde{d}'_{m,n,q}^{(2,3)} = \frac{1}{I_m(q_n b_3)} \left\{ \frac{q_n}{2} d_{2,0,n_r}^{(2,3)} \left(d_{m-1,n,q}^{(2,3)} + d_{m+1,n,q}^{(2,3)} \right) + mn_r d_{1,0,n_r}^{(2,3)} d_{m,n,q}^{(2,3)} \right\} \quad (n > 0) \tag{A51}$$

$$\tilde{e}_{0,0,q}^{(2,3)} = e_{0,0,q}^{(2,3)} \quad (m = 0, n = 0), \quad \tilde{e}'_{m,0,q}^{(2,3)} = \frac{e_{m,0,q}^{(2,3)}}{a_2^{-|m|}} \quad (m \neq 0, n = 0) \tag{A52}$$

$$\tilde{e}_{m,n,q}^{(2,3)} = \frac{e_{m,n,q}^{(2,3)}}{K_m(q_n a_2)} \quad (n > 0) \tag{A53}$$

$$\tilde{e}'_{0,0,q}^{(2,3)} = -d_{2,0,n_r}^{(2,3)} e_{1,0,q}^{(2,3)} \quad (m = 0, n = 0) \tag{A54}$$

$$\tilde{e}'_{m,0,q}^{(2,3)} = \frac{1}{a_2^{-|m|}} \left(-|m| d_{1,0,n_r}^{(2,3)} e_{m,0,q}^{(2,3)} + mn_r d_{1,0,n_r}^{(2,3)} e_{m,0,q}^{(2,3)} \right) \quad (m \neq 0, n = 0) \tag{A55}$$

$$\tilde{e}'_{m,n,q}^{(2,3)} = \frac{1}{K_m(q_n a_2)} \left\{ -\frac{q_n}{2} d_{2,0,n_r}^{(2,3)} \left(e_{m-1,n,q}^{(2,3)} + e_{m+1,n,q}^{(2,3)} \right) + mn_r d_{1,0,n_r}^{(2,3)} e_{m,n,q}^{(2,3)} \right\} \quad (n > 0) \tag{A56}$$

$$\tilde{f}_{m,0,q}^{(3)} = \frac{f_{m,0,q}^{(3)}}{H_m(k a_3)} \quad (n = 0), \quad \tilde{f}'_{m,n,q}^{(3)} = \frac{f_{m,n,q}^{(3)}}{K_m(k_n a_3)} \quad (n > 0) \tag{A57}$$

$$\tilde{f}'_{m,0,q}^{(3)} = \frac{1}{H_m(k a_3)} \left\{ \frac{k}{2} d_{2,0,n_r}^{(3)} \left(f_{m-1,0,q}^{(3)} - f_{m+1,0,q}^{(3)} \right) + mn_r d_{1,0,n_r}^{(3)} f_{m,0,q}^{(3)} \right\} \quad (n = 0) \tag{A58}$$

$$\tilde{f}'_{m,n,q}^{(3)} = \frac{1}{K_m(k_n a_3)} \left\{ -\frac{k_n}{2} d_{2,n,n_r}^{(3)} \left(f_{m-1,n,q}^{(3)} + f_{m+1,n,q}^{(3)} \right) + mn_r d_{1,n,n_r}^{(3)} f_{m,n,q}^{(3)} \right\} \quad (n > 0) \tag{A59}$$

References

1. Wang, C.M.; Wang, B. *Large Floating Structures*; Springer: Singapore, 2015; Volume 3.
2. Wang, C.M.; Lim, S.H.; Tay, Z.Y. *WCFS2019: Proceedings of the the World Conference on Floating Solutions*; Springer: Singapore, 2020.
3. Piątek, Ł.; Lim, S.H.; Wang, C.M.; Graaf-van Dinther, R. *WCFS2020: Proceedings of the the Second World Conference of Floating Solutions, Rotterdam*; Springer: Singapore, 2022.
4. Miloh, T. Wave loads on a floating solar pond. In *The Proceedings, International Workshop on Ship and Platform Motions*; Yeung, R.W., Ed.; University of California: Berkeley, CA, USA, 1983.
5. Wang, C.M.; Chu, Y.I.; Park, J.C. Moving offshore for fish farming. *J. Aquac. Mar. Biol.* **2019**, *8*, 38–39. [[CrossRef](#)]
6. McNow, J.S. 18. Waves and Seiche in Idealized Ports. In *Proceedings of NBS Semicentennial Symposium on Gravity Waves Held at the NBS on June 18–20, 1951*; National Bureau of Standards Circular 521: Washington, DC, USA, 1952; pp. 153–164.
7. Miles, J.; Munk, W. Harbor paradox. *J. Waterw. Harb. Div.* **1961**, *87*, 111–132. [[CrossRef](#)]
8. Garrett, C. Bottomless harbours. *J. Fluid Mech.* **1970**, *43*, 433–449. [[CrossRef](#)]
9. Fernandes, A.C. *Analysis of an Axisymmetric Pneumatic Buoy by Reciprocity Relations and a Ring-Source Method*; Massachusetts Institute of Technology: Cambridge, MA, USA, 1983.
10. Konispoliatis, D.; Mazarakos, T.; Mavrakos, S. Hydrodynamic analysis of three-unit arrays of floating annular oscillating-water-column wave energy converters. *Appl. Ocean Res.* **2016**, *61*, 42–64. [[CrossRef](#)]
11. Mavrakos, S. Wave loads on a stationary floating bottomless cylindrical body with finite wall thickness. *Appl. Ocean Res.* **1985**, *7*, 213–224. [[CrossRef](#)]
12. Mavrakos, S. Hydrodynamic coefficients for a thick-walled bottomless cylindrical body floating in water of finite depth. *Ocean Eng.* **1988**, *15*, 213–229. [[CrossRef](#)]
13. Mavrakos, S.A.; Chatjigeorgiou, I.K. Second-order hydrodynamic effects on an arrangement of two concentric truncated vertical cylinders. *J. Mar. Struct.* **2009**, *22*, 545–575. [[CrossRef](#)]

14. Mavrakos, S.A. Hydrodynamic coefficients in heave of two concentric surface-piercing truncated circular cylinders. *Appl. Ocean Res.* **2004**, *26*, 84–97. [[CrossRef](#)]
15. Mavrakos, S.A. Hydrodynamic characteristics of two concentric surface-piercing. *Mitochondrial Med.* **2006**, 221–228.
16. Mavrakos, S.A.; Katsaounis, G.M.; Chatjigeorgiou, I.K. Performance characteristics of a tightly moored piston-like wave energy converter under first-and second-order wave loads. In *International Conference on Offshore Mechanics and Arctic Engineering*; AMSE: Estoril, Portugal, 2008; pp. 783–792.
17. Wetmore, S.B.; Ramsden, H.D. CIDS: A Mobile Concrete Island Drilling System for Arctic Offshore Operations. *Mar. Technol. SNAME News* **1984**, *21*, 1–11. [[CrossRef](#)]
18. Fishfarmexpert. FjordMAX Promises More Fish and Smaller Footprint. Available online: <https://www.fishfarmingexpert.com/article/fjordmax-promises-more-fish-and-smaller-footprint/> (accessed on 25 July 2022).
19. Wang, P.; Zhao, M.; Du, X.; Liu, J. Analytical solution for the short-crested wave diffraction by an elliptical cylinder. *Eur. J. Mech.-B/Fluids* **2019**, *74*, 399–409. [[CrossRef](#)]
20. Park, J.C.; Wang, C.M. Hydrodynamic behaviour of floating polygonal platforms under wave action. *J. Mar. Sci. Eng.* **2021**, *9*, 923. [[CrossRef](#)]
21. Park, J.C.; Wang, C. Hydrodynamic behaviour of floating polygonal ring structures under wave action. *Ocean Eng.* **2022**, *249*, 110195. [[CrossRef](#)]
22. Mansour, A.M.; Williams, A.N.; Wang, K. The diffraction of linear waves by a uniform vertical cylinder with cosine-type radial perturbations. *Ocean Eng.* **2002**, *29*, 239–259. [[CrossRef](#)]
23. Liu, J.; Guo, A.; Li, H. Analytical solution for the linear wave diffraction by a uniform vertical cylinder with an arbitrary smooth cross-section. *Ocean Eng.* **2016**, *126*, 163–175. [[CrossRef](#)]
24. Liu, J.; Guo, A.; Fang, Q.; Li, H.; Hu, H.; Liu, P. Investigation of linear wave action around a truncated cylinder with non-circular cross section. *J. Mar. Sci. Technol.* **2018**, *23*, 866–876. [[CrossRef](#)]